micro

MDPI

Review

Chitosan Films for Micro- and Nanosensors: A Systematic Evidence Map and Curated Critical Review of Functional Roles, Transduction, and Device Readiness

Muhammad Rif'an [1,*], Arie Aryanto [2], Karlisa Priandana [3] and Waras Nurcholis [4]

[1] Information Systems Study Program, Faculty of Science and Technology, Universitas Terbuka, South Tangerang 15418, Indonesia
[2] Biology Study Program, Faculty of Science and Technology, Universitas Terbuka, South Tangerang 15418, Indonesia; arie.aryanto@ecampus.ut.ac.id
[3] Computer Science Study Program, School of Data Science, Mathematics and Informatics, IPB University, Bogor 16680, Indonesia; karlisa@apps.ipb.ac.id
[4] Department of Biochemistry, Faculty of Mathematics and Natural Sciences, IPB University, Bogor 16680, Indonesia; wnurcholis@apps.ipb.ac.id
* Correspondence: m.rifan@ecampus.ut.ac.id

Abstract

Chitosan films and interfaces are increasingly used in micro- and nanosensors, yet the contribution of chitosan is often obscured by hybrid architectures. This systematic evidence map and curated critical review evaluated fabrication routes, micro-/nanoscale structures, functional roles, transduction mechanisms, analytical validation, reporting completeness, and device readiness. Searches of Scopus, PubMed, and IEEE Xplore yielded 15,058 database records. After deduplication, 8832 unique database-derived records underwent rule-based evidence mapping: Core Primary Candidate (n = 2617), Contextual Evidence (n = 3096), Manual Review (n = 1318), and Exclude (n = 1801). A separately assembled curated full-text subset contained 73 unique records, including 32 unique additions to the database-derived corpus. Full-text adjudication of this curated subset identified 26 studies meeting the strict CORE criteria, 17 boundary experimental studies, eight contextual experimental/material studies, 18 review/contextual sources, two methodological sources, and two exclusions. The detailed critical synthesis and reporting-completeness assessment were restricted to the 26 CORE studies assessed within this curated subset and should not be interpreted as an exhaustive synthesis of all 2617 automated candidate records. Within the 26-study curated CORE subset, reporting completeness was highest for response definition (26/26, 100.0%) and functional-role reporting (25/26, 96.2%), but lower for chitosan identity and selectivity/interference (17/26, 65.4% each) and stability (13/26, 50.0%). The assessed studies indicate that strong analytical performance in hybrid architectures generally reflected the complete sensing system rather than chitosan alone. The proposed role–structure–transduction–evidence framework supports clearer component attribution, within-platform comparison, validation, and device-readiness assessment within the evidence set examined.

Keywords: chitosan films; micro- and nanosensors; functional interfaces; electrochemical sensors; optical sensors; gravimetric sensors; humidity sensors; device readiness

Check for updates

Academic Editor: Yang Zou

Received: 7 August 2026
Revised: 21 September 2026
Accepted: 22 September 2026
Published: 24 September 2026

Copyright: © 2026 by the authors. Licensee MDPI, Basel, Switzerland. This article is an open access article distributed under the terms and conditions of the Creative Commons Attribution (CC BY) license.

1. Introduction

Sensor systems are essential to food safety, environmental monitoring, clinical analysis, industrial process control, and wearable health applications. However, many sensing devices continue to rely on persistent polymer substrates, resource-intensive functional modifiers, and fabrication routes whose environmental impacts are rarely evaluated systematically [1]. In this context, chitosan is attractive not merely as a biodegradable alternative, but as a processable functional material capable of interacting with analytes, supporting recognition elements, and hosting signal-generating components.

Chitosan is produced through the deacetylation of chitin and contains abundant amino and hydroxyl groups. These functional groups enable protonation, hydrogen bonding, metal coordination, chemical modification, and biomolecule immobilization [2–6]. Its molecular weight and degree of deacetylation influence solution viscosity, amino-group density, swelling behavior, adhesion, and mechanical integrity [2,6]. These properties can directly affect film formation and sensor response. Nevertheless, molecular weight, degree of deacetylation, and related physicochemical characteristics are frequently mentioned without being adequately measured, controlled, or reported in sensor studies.

At the micro- and nanoscale, chitosan has been processed as thin coatings, electrodeposited layers, nanofibrous mats, composite films, self-assembled interfaces, and modifiers of patterned electrodes or resonant structures. It has been incorporated into electrochemical and impedimetric interfaces [7–23], optical, fluorescent, and colorimetric films [24–42], chemiresistive, electrochemical, and optical gas-sensing devices [43–50], capacitive and resistive humidity sensors [51–58], quartz crystal microbalances (QCMs) [59], and microelectromechanical-system (MEMS) cantilevers and resonators [60–62]. These platforms rely on different physical principles and therefore require platform-specific definitions of sensitivity, selectivity, response time, recovery, stability, hysteresis, and analytical performance.

A central challenge in interpreting this literature is the attribution of functional roles. Chitosan may act as the analyte-responsive phase, a recognition or analyte-partitioning matrix, an immobilization or binder layer, or a structural support for another active material. Accordingly, a low detection limit obtained using an aptamer, enzyme, metal oxide, fluorescent probe, nanocarbon, field-effect transistor, or resonator cannot be attributed to chitosan alone without appropriate control experiments. Conversely, in humidity and gravimetric sensing, water uptake, swelling, ionic transport, and viscoelastic loading may make chitosan directly responsible for the measured response. Distinguishing these roles is therefore necessary for meaningful comparison among devices.

Previous reviews have generally focused on individual application domains. Electrochemical chitosan sensors have been reviewed from the perspectives of nanocomposites, biosensing, molecular imprinting, food safety, pharmaceuticals, and clinical analysis [7,63–67]. Other reviews have addressed biomedical nanosensors and hydrogel-based bioelectronic sensing [68,69], optical heavy-metal sensing [70], intelligent and colorimetric food packaging [71–76], flexible electronics and biodegradable or transient electronics [77,78], and mobile-phone-based biosensing [79]. However, these studies have not applied a common framework for distinguishing the functional contribution of chitosan from that of receptors, fillers, nanostructures, and transducer amplification.

A systematic synthesis is therefore needed to connect chitosan properties and film architecture with functional role, transduction mechanism, analytical validation, and device readiness. The reporting of this systematic evidence map and critical review was informed by the Preferred Reporting Items for Systematic Reviews and Meta-Analyses (PRISMA) 2020 framework [80,81]. It distinguishes primary experimental device studies from review and contextual literature and organizes the evidence according to the measured quantity,

transduction mechanism, and dominant role of chitosan rather than by application category alone. This approach enables comparisons across electrochemical, optical, chemiresistive, gravimetric, humidity-sensing, resonant, and microelectromechanical platforms while preserving the technical differences among them.

Unlike previous application-specific reviews, the present work separates material composition from sensing mechanism and evaluates chitosan according to its dominant functional role, transduction domain, validation evidence, and device-readiness level.

The objectives of this review are to: (i) compare fabrication routes and the resulting micro- and nanostructures; (ii) distinguish the contribution of chitosan from those of fillers, receptors, transducers, and environmental conditions; (iii) evaluate platform-specific performance metrics and validation requirements; and (iv) propose actionable criteria for reproducibility, device readiness, and defensible sustainability claims. Figure 1 summarizes the scope and analytical framework adopted in this review.

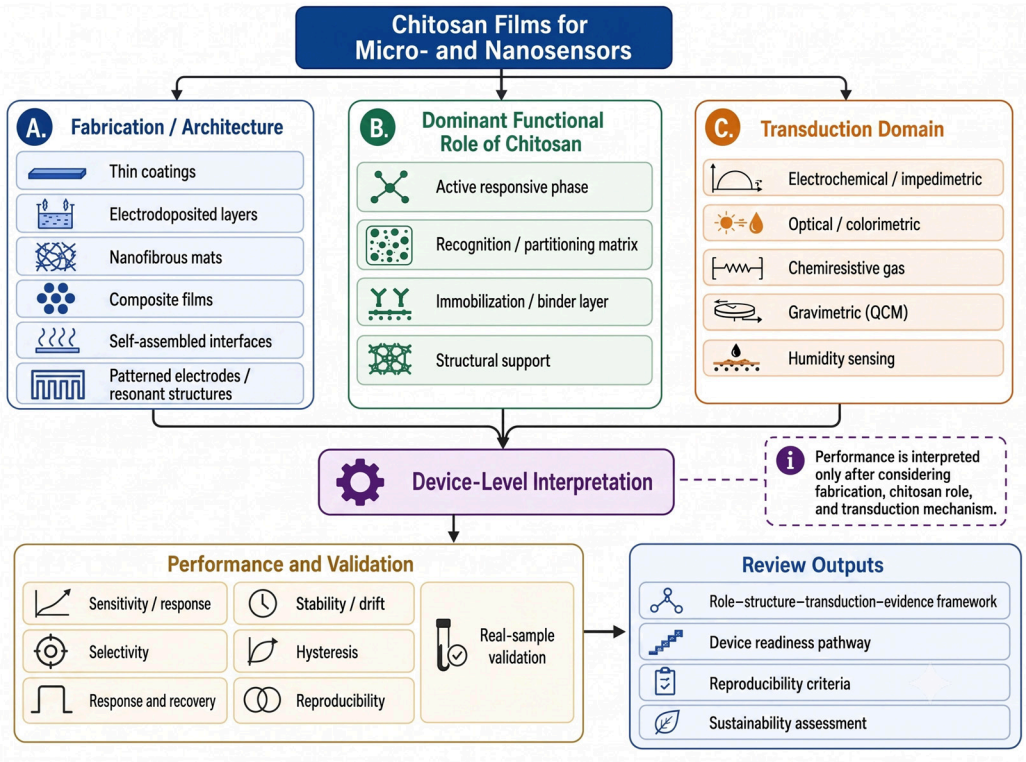


Figure 1. Scope and analytical taxonomy of the review. Chitosan films are classified according to fabrication route and architecture, dominant functional role, and transduction domain used in the main synthesis before their performance is interpreted at the device level.

2. Materials and Methods

2.1. Review Design and Reporting Framework

This study combined a systematic evidence-mapping approach with a curated critical qualitative review of chitosan films and interfaces used in micro- and nanoscale sensing devices. The evidence map was designed to characterize the breadth of the database-derived literature, identify potentially relevant experimental and contextual records, and evaluate the distribution of sensing platforms. The detailed qualitative synthesis was conducted separately using a curated full-text subset and was structured around fabrication route, film architecture, the dominant functional role of chitosan, transduction mechanism, analytical validation, and device readiness. The curated synthesis was not intended to represent exhaustive full-text screening of all automatically classified candidate records.

Reporting was informed by the Preferred Reporting Items for Systematic Reviews and Meta-Analyses (PRISMA) 2020 statement and its explanation and elaboration document [80,81]. Because title and abstract classification was performed through rule-based automation and the final qualitative evidence set was curated separately, the study-selection workflow is reported as an evidence-identification and reconciliation process rather than as a conventional manually screened systematic-review pathway.

The core qualitative synthesis focused on primary experimental studies in which chitosan or a chitosan derivative formed a film, coating, membrane, nanofibrous layer, composite layer, self-assembled interface, or functional layer on a miniaturized transducer. Eligible platforms included electrochemical, impedimetric, optical, colorimetric, chemiresistive, conductometric, gravimetric, capacitive, resistive, resonant, and field-effect-transistor devices.

2.2. Protocol and Registration

The review protocol was retrospectively registered in the Open Science Framework Registries under DOI: 10.17605/OSF.IO/YDUK9. The registration documented the review scope, research questions, eligibility concepts, functional classification of chitosan, extraction domains, and narrative-synthesis framework.

Several refinements were introduced after the initial protocol was prepared. These included broader coverage of gravimetric sensing, quartz crystal microbalances, microcantilevers, resonators, microelectromechanical systems, and nanoelectromechanical systems, as well as the implementation of rule-based automated evidence mapping. These deviations are reported transparently and were retained in the archived review documentation.

2.3. Research Questions

The review addressed the following research questions:

RQ1. Which fabrication routes and micro- and nanoscale film architectures have been used in chitosan-based sensing devices?

RQ2. What functional role does chitosan perform in each device, and which material or structural variables are associated with sensor performance?

RQ3. How should performance be compared within electrochemical, optical, chemiresistive, gravimetric, resonant, and humidity-sensing domains?

RQ4. Which methodological weaknesses limit attribution of chitosan-specific effects, reproducibility, comparability, and practical deployment?

RQ5. What reporting and validation pathway is required to support device readiness and defensible sustainability claims for chitosan-based sensors?

2.4. Information Sources and Search Strategy

Systematic searches were conducted in Scopus, PubMed, and IEEE Xplore from database inception to 4 August 2026. The database searches were supplemented by backward and forward citation tracking, publisher-platform searching, and a manually curated Mendeley Reference Manager library (Elsevier, Amsterdam, The Netherlands) compiled during the review process.

Scopus and PubMed were each searched using two complementary query blocks. The first block emphasized chitosan films, coatings, membranes, sensing interfaces, and established sensor-transduction terminology. The second block targeted micro- and nanoscale materials and device architectures, including microsensors, nanosensors, microelectrodes, nanoelectrodes, microcantilevers, interdigitated electrodes, microelectromechanical systems (MEMS), nanoelectromechanical systems (NEMS), quartz crystal microbalances (QCMs), resonators, field-effect transistors, nanofibers, nanorods, nanowires, nanoparticles, and nanocomposites.

IEEE Xplore was searched using the All-Metadata field. The results were restricted to journal articles, conference publications, and early access articles, whereas books were excluded. The final IEEE Xplore search identified 272 records before internal deduplication.

The database-specific search strategies combined three principal concept groups:

- chitosan-related terms, including chitosan, chitosan-based, chitosan film, coating, membrane, composite, and nanocomposite;
- sensing and transduction terms, including sensor, biosensor, chemosensor, electrochemical, impedimetric, optical, fluorescent, colorimetric, gas sensor, humidity sensor, gravimetric, QCM, microcantilever, resonator, MEMS, NEMS, and field-effect transistor;
- interface and architecture terms, including thin film, layer, electrode, sensing interface, microelectrode, nanofiber, nanorod, nanowire, and interdigitated electrode.

The complete database-specific search strings, searched fields, filters, search dates, and record counts are provided in Supplementary Table S1. Searches were restricted to English-language records, and no publication-year restriction was applied.

The two Scopus searches identified 10,765 records before cross-query deduplication, while the two PubMed searches identified 4021 records. The filtered IEEE Xplore search identified 272 records. The three electronic databases therefore contributed 15,058 records. Supplementary searching and the curated Mendeley library yielded 73 references that were reconciled separately because 41 overlapped the database-derived corpus and 32 were unique additions. Reconciliation with the 32 unique additions therefore yielded a combined corpus of 8864 unique records.

2.5. Eligibility Criteria

Studies were eligible for the strict CORE synthesis only when all of the following criteria were met:

1. the study reported original experimental research;
2. chitosan or a chitosan derivative formed a film, coating, membrane, nanofibrous layer, composite layer, self-assembled interface, or other functional sensing layer;
3. the chitosan-containing material had a defined sensing, recognition, analyte-partitioning, indicator, immobilization, or signal-coupling function;
4. a micro- or nanoscale material, structure, film, interface, or transducer was functionally integral to analyte recognition, analyte–interface interaction, or signal transduction;
5. at least one device-relevant material, analytical, or operational outcome was reported.

Eligible outcomes included film or interface structure, electrical or optical response, sensitivity, response equation, limit of detection, linear range, selectivity, response and recovery time, hysteresis, repeatability or reproducibility, drift, stability, or real-sample or field-relevant validation.

Studies were excluded from the strict CORE synthesis when chitosan was used exclusively for adsorption, treatment, delivery, wound care, tissue engineering, scaffold fabrication, antimicrobial activity, separation, or bulk material characterization without a sensing endpoint. Macroscale intelligent-packaging films and other sensing studies without a functionally integral micro-/nanoscale feature were retained, where relevant, as contextual or boundary evidence rather than counted as CORE.

Patents, editorials, commentaries, retracted publications, duplicate records, and reports without sufficient information to determine the sensing function or device configuration were excluded. Review articles, general chitosan-property studies, methodological references, and sustainability studies were retained as contextual or methodological sources but were not counted as CORE primary studies.

Operationally, a micro- or nanosensor was defined as a sensing system in which a micro- or nanoscale material, structure, film, interface, or transducer was functionally integral to analyte recognition, analyte–interface interaction, or signal transduction. The mere presence of nanoparticles, nanofillers, or other nanoscale additives in an otherwise macroscale film was not sufficient for CORE inclusion unless that feature directly participated in the sensing mechanism or device architecture.

For full-text adjudication of the curated records, the eligibility criteria were applied sequentially. A record was classified as CORE only when all five criteria above were satisfied: original experimental research; a functional chitosan-containing sensing film or interface; an explicit sensing-related role for chitosan; a functionally integral micro-/nanoscale material, structure, film, interface, or transducer; and at least one device-relevant outcome. Records that otherwise described experimental sensing systems but did not satisfy the strict micro-/nanoscale criterion were retained as boundary experimental or contextual experimental/material evidence, as appropriate. Reviews and methodological papers were classified separately, and records without qualifying chitosan sensing relevance were excluded. Record-level classifications and adjudication rationales are provided in Supplementary Table S4.

2.6. Record Management, Automated Evidence Mapping, and Curated Evidence Selection

Database exports were processed within a common record-management workflow. Exact duplicates were identified using normalized digital object identifiers, PubMed identifiers, source identifiers, and normalized titles. Potential near-duplicate records were additionally examined using title-similarity procedures.

The electronic database searches produced 15,058 records. After removal of 6226 duplicates within and across Scopus, PubMed, and IEEE Xplore, 8832 unique database-derived records remained. The manually curated Mendeley library contained 73 unique references after consolidation of one duplicate full-text record. Of these, 41 were already represented in the database-derived corpus, and 32 were unique additions. Reconciliation therefore produced a combined corpus of 8864 unique records.

The 8832 database-derived records underwent rule-based automated evidence mapping implemented through a predefined computational script written in Python 3.12.3 (Python Software Foundation, Wilmington, DE, USA) and executed under Ubuntu 24.04.4 LTS within Windows Subsystem for Linux (WSL; Microsoft Corporation, Redmond, WA, USA). The script evaluated titles, abstracts, keywords, document types, database origins, and bibliographic identifiers against prespecified signals for chitosan, sensing function, film/interface configuration, micro-/nanoscale terminology, transduction mechanism, experimental performance, and non-sensing exclusions.

The script assigned each database-derived record to one of four mutually exclusive evidence-mapping strata: Core Primary Candidate, Contextual Evidence, Manual Review, or Exclude. These strata were designed for reproducible bibliographic mapping and were not treated as final study-level eligibility decisions.

Of the 8832 database-derived records, 2617 were classified as Core Primary Candidate, 3096 as Contextual Evidence, 1318 as Manual Review, and 1801 as Exclude. The automated classifications were retained without manual modification. The 1801 Exclude records were reported as automated title/abstract exclusions; the other three categories remained evidence-map strata.

The curated Mendeley library was assembled during the review process from supplementary searching, backward and forward citation tracking, publisher-platform searching, and records previously collected for this topic. It was used as a supplementary, purposively curated full-text subset for detailed mechanistic and reporting-level assessment rather than

as a substitute for the reproducible database searches. The 73 curated records were not selected through exhaustive full-text screening of all 2617 records classified automatically as Core Primary Candidate.

All 73 unique curated records underwent structured full-text adjudication against the strict operational criteria described in Section 2.5. The final inventory comprised 26 studies meeting the CORE criteria, 17 boundary experimental studies, eight contextual experimental/material studies, 18 review/contextual sources, two methodological sources, and two exclusions. Accordingly, the 26 CORE studies represent studies meeting the strict criteria within the curated subset and should not be interpreted as the complete set of all potentially eligible studies in the broader automated evidence map. Only these 26 assessed CORE studies contributed to the reporting-completeness matrix and detailed critical performance synthesis; boundary and contextual records were used only where explicitly identified as supporting interpretation.

Complete database exports, deduplication outputs, automated classification rules, the 73-record final adjudication inventory, and the 26-study extraction matrix with evidence-line provenance were retained as Supplementary Materials.

2.7. Data Extraction and Functional Classification

A standardized study-level extraction matrix was completed for the 26 CORE studies. It recorded bibliographic information; chitosan source and specification; molecular weight and degree of deacetylation where reported; derivative or crosslinker; formulation and deposition conditions; film/interface structure; substrate and transducer geometry; filler or recognition element; analyte and sample matrix; transduction mechanism; response definition; operating conditions; analytical range and sensitivity; limit of detection; dynamic response; selectivity/interference; repeatability or reproducibility; stability; and real-sample or field-relevant validation. Information not explicitly reported in the original full text was recorded as not reported and was not inferred from related studies, manufacturer specifications, or secondary sources.

The functional contribution of chitosan was classified into four non-exclusive roles: active analyte- or environmentally responsive phase, recognition or analyte-partitioning matrix, immobilization or binder layer, and structural or composite support. The dominant signal-generating component was recorded separately to avoid assigning performance arising from receptors, fillers, nanostructures, transducer geometry, or amplification mechanisms to chitosan alone. Throughout the review, film/interface is used as the generic umbrella term; coating, layer, membrane, and related terms are retained only when they describe the architecture reported in the original study.

The reporting of a functional role was distinguished from experimental demonstration of a causal contribution. A study was considered to report the role of chitosan when the stated function of chitosan was differentiated from that of the receptor, filler, catalytic material, transducer, or amplification mechanism. Stronger causal evidence required a matched control or controlled comparison capable of isolating the effect of chitosan, such as a chitosan-free interface, an alternative matrix, systematic variation in chitosan composition, or an equivalent control architecture.

2.8. Data Synthesis

A quantitative meta-analysis was not performed because the 26 CORE studies differed substantially in analytes, concentration units, response definitions, operating conditions, relative-humidity ranges, device geometries, film/interface architectures, and validation procedures. Structured narrative synthesis was conducted across electrochemical/impedimetric, optical/colorimetric/fiber-optic, gas/gravimetric, and humidity-sensing

domains. Evidence from boundary and contextual records was not pooled with CORE performance results.

Cross-platform interpretation followed the proposed role–structure–transduction–evidence framework. Numerical comparisons were made only when the original studies reported sufficiently comparable response definitions, units, operating conditions, and calibration procedures. Results obtained using incompatible definitions or experimental conditions were classified as not directly comparable. Qualitative descriptions such as "high sensitivity", "rapid response", or "good stability" were not treated as equivalent evidence unless they were supported by clearly defined metrics and appropriate comparators.

2.9. Descriptive Assessment of Reporting Completeness

Because no single validated risk-of-bias or quality-assessment instrument was considered suitable for the heterogeneous combination of materials-science experiments, analytical-chemistry studies, and sensor-device investigations, reporting completeness was assessed descriptively across ten prespecified domains. These domains covered chitosan identity, fabrication reproducibility, film or interface characterization, functional-role reporting, response definition, operating conditions, selectivity or interference testing, repeatability or reproducibility, stability, and application validation.

The domains were used as a narrative interpretive checklist and were not combined into a numerical quality score or formal risk-of-bias classification. Table 1 presents the minimum information considered necessary for adequate reporting within each domain.

Table 1. Reporting-completeness domains used to assess the 26-study curated CORE subset.

Domain	Criterion for Adequate Reporting
Chitosan identity	The source and at least one relevant specification, such as molecular weight, degree of deacetylation, or material grade, were reported
Fabrication reproducibility	Chitosan concentration, solvent, deposition parameters, and drying or post-treatment conditions were reported
Film/interface characterization	Film thickness, morphology, porosity, or another relevant structural property was measured using an appropriate method
Functional-role reporting	The stated functional role of chitosan was distinguished from that of the receptor, filler, transducer, or amplification mechanism; this reporting criterion did not by itself require experimental demonstration of causality
Response definition	The response equation or an unambiguous signal definition was provided
Operating conditions	Analyte concentration, temperature, relative humidity, and other relevant operating parameters were reported
Selectivity/interference	Relevant competing analytes, environmental interferents, or mixed-condition tests were examined
Repeatability/reproducibility	Repeated cycles, replicate preparations, or measurements across multiple devices were reported
Stability	Drift, shelf life, long-term operation, storage stability, or mechanical stability was assessed
Application validation	Real samples, realistic exposure conditions, or a field-relevant demonstration was included

For each CORE study, every reporting domain was coded as 1 (criterion satisfied) or 0 (criterion not satisfied), with NA reserved for genuinely non-applicable domains and excluded from the denominator. Platform relevance was considered when interpreting operating conditions; for example, relative humidity was not required for an aqueous electrochemical assay when it was not mechanistically relevant. No NA assignments were required in the final 26-study matrix. Supporting full-text line references and adjudication notes were retained for every decision. Frequencies and percentages were calculated using the 26 CORE studies assessed within the curated full-text subset as the denominator.

2.10. Scope and Methodological Boundaries

The review was restricted to English-language reports involving chitosan sensing films or interfaces. Citation tracking, publisher-platform searching, and the curated Mendeley library were supplementary identification methods. The strict CORE synthesis was intentionally narrower than the broader contextual literature: macroscale smart-packaging indicators, nanoscale additives that were incidental to sensing, and devices lacking a functionally integral micro-/nanoscale feature were not counted as CORE.

The evidence base included heterogeneous proof-of-concept devices with different architectures, response equations, analytical units, environmental conditions, and levels of validation. The review therefore emphasized component-specific attribution, within-platform comparability, reporting completeness, and device-readiness gaps rather than ranking all devices using a single performance measure.

The rule-based evidence map enabled reproducible processing of the large bibliographic corpus, whereas the curated full-text audit established the final study-level scope. Neither the automated mapping nor the 73-record full-text adjudication was independently duplicated by a second reviewer; this limitation is considered in Section 4.6.

The protocol was registered retrospectively, and the curated library was not produced by full-text screening of all 2617 automated Core Primary Candidate records. All selection rules, final record classifications, extraction decisions, and provenance were therefore retained to make the scope and reviewer judgment auditable.

2.11. Generative AI-Assisted Figure Preparation

The scientific content, structure, terminology, numerical values, and logical relationships presented in Figures 1–5 were developed manually by the authors in Microsoft PowerPoint (Microsoft Corporation, Redmond, WA, USA). Google Gemini (Google LLC, Mountain View, CA, USA) was subsequently used to assist with graphical refinement and the addition of scientific illustrative elements. Initial graphical refinement was performed using Gemini 3.5, followed by Gemini 3.6 Reasoning during subsequent refinement of the figures. The AI-assisted tasks were limited to improvements in layout, typography, iconography, spacing, alignment, proportions, scientific illustrations, and overall visual presentation. The prompts instructed the AI tool to preserve the author-prepared scientific content and not to introduce new scientific claims or modify the underlying data, numerical values, methodology, interpretations, or conclusions. All AI-assisted outputs were reviewed and verified by the authors for scientific accuracy, and the authors take full responsibility for the final figures.

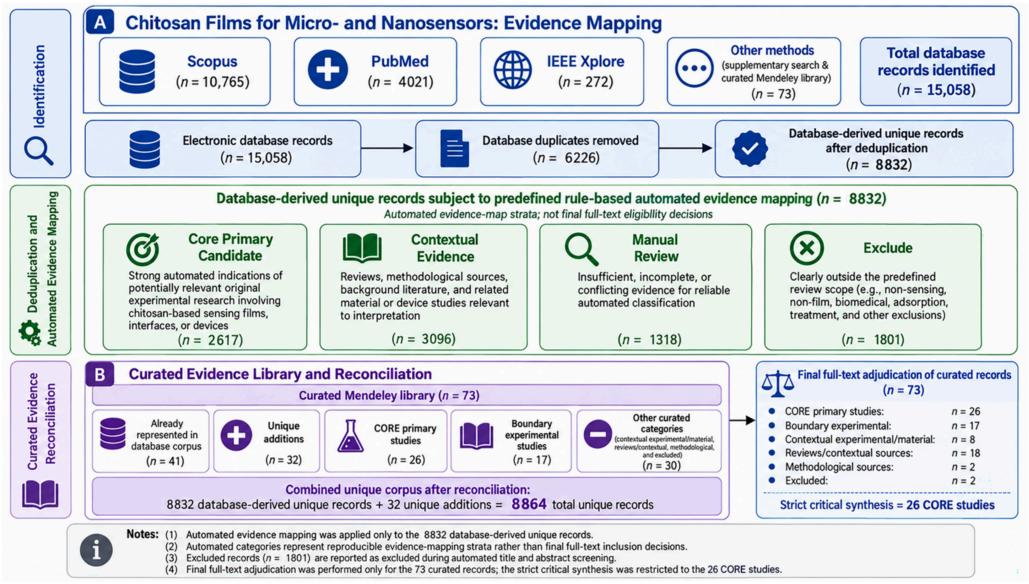


Figure 2. Evidence identification, automated mapping, curated-library reconciliation, and final full-text adjudication. Electronic searches yielded 15,058 records; 6226 duplicates were removed, leaving 8832 unique database-derived records for rule-based mapping. The 73 curated references were reconciled separately: 41 overlapped the database corpus, and 32 were unique additions, producing 8864 unique records after reconciliation. Full-text audit of the curated subset identified 26 studies meeting the CORE criteria, 17 boundary experimental studies, eight contextual experimental/material studies, 18 review/contextual sources, two methodological sources, and two exclusions. The detailed critical synthesis used the 26 CORE studies assessed within this curated subset; this subset was not intended as an exhaustive full-text screening of all automated candidate records.

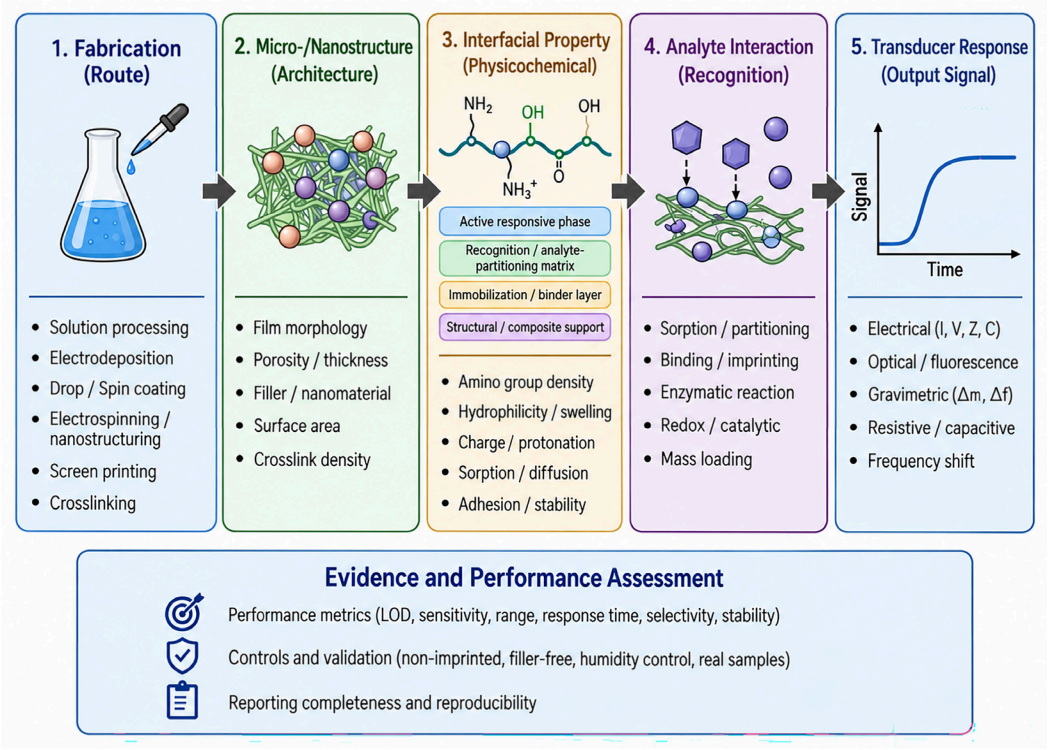


Figure 3. Role–structure–transduction–evidence framework used to interpret the contribution of chitosan films and interfaces in micro- and nanosensor architectures.

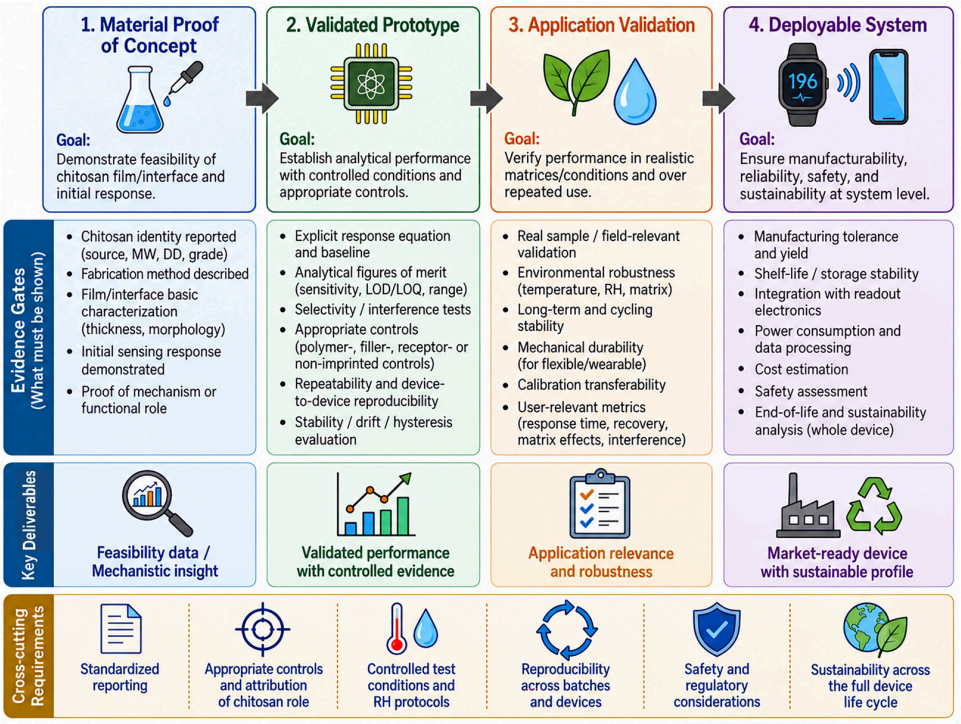


Figure 4. Proposed device-readiness pathway and evidence gates for chitosan-film micro- and nanosensors. Progression from material proof of concept to a deployable system requires increasingly rigorous evidence for material identity, fabrication reproducibility, analytical validation, realistic application testing, manufacturing tolerance, stability, cost, safety, and end-of-life management.

Transduction Domain	1. Electrochemical / Impedimetric	2. Optical / Fluorescent / Colorimetric	3. Chemiresistive / Conductometric (Gas / VOC)	4. Gravimetric (QCM Resonator)	5. Capacitive / Resistive / FET (Humidity)
Evidence status in strict synthesis	CORE represented	CORE represented	Predominantly boundary / contextual	CORE represented	CORE represented
Typical measured quantity	Current (I), Potential (E), Impedance (Z), Charge transfer	Intensity (I), Absorbance (A), Reflectance (R), Color (RGB/ΔE)	Resistance (R), Conductance (G), Voltage (V) change	Mass loading (Δm), Frequency shift (Δf), Resonant freq. change (Δf_r)	Capacitance (C), Resistance (R), Gate current (I_g), Threshold shift (ΔV_{th})
Typical role of chitosan	Film former, receptor immobilization, imprinting matrix, ionomer	Probe / dye host, nanoparticle or enzyme immobilization, optical matrix	Sorption / partitioning layer, binder for metal oxides or nanostructures	Mass-sensitive layer, swelling layer	Dielectric and ionic matrix, moisture-responsive layer
Dominant confounders	Fouling, solution resistance, pH, ionic strength, receptor contribution	Photobleaching, inner filter, pH, ionic strength, probe stability	Humidity, temperature, baseline drift, grain-boundary effects, contact resistance	Temperature, non-target sorption, viscoelastic damping, packaging effects	Temperature, RH hysteresis, electrode geometry, ion leaching
Minimum validation to support a claim	• Response equation • Calibration range • Selectivity / interference • Repeatability • Stability / drift • Real-sample test	• Response equation • Calibration range • Selectivity / interference • Repeatability • Stability (photo/chemical) • Real-sample test	• Response equation • Humidity control • Target-only and humidity-only tests • Mixed-gas tests • Repeatability • Stability / drift	• Response equation • Temperature control • Non-target sorption • Repeatability • Stability • Realistic application test	• Response equation • RH control & protocol • Hysteresis evaluation • Repeatability • Stability / drift • Mechanical tests (if flexible / wearable)
Comparability note	Compare only with studies using similar cell design, electrolyte, potential window, and response definition.	Compare only with studies using similar optical setup, excitation/illumination, and color-calibration method.	Compare only with studies using similar temperature, RH, gas mixture, and response definition.	Compare only with studies using similar resonant temperature, packaging, and response definition.	Compare only with studies using similar RH range, frequency/voltage, geometry, and response definition.

Evidence status differs across domains; only studies meeting the strict operational micro-/nanosensor definition contributed to the 26-study CORE synthesis.

Figure 5. Cross-platform comparability, evidence status, and minimum-validation matrix. Evidence status differs among transduction domains; only studies meeting the strict operational micro-/nanosensor definition contributed to the 26-study CORE synthesis. Numerical comparison is appropriate only when response equations, measurement units, environmental conditions, calibration procedures, and device geometries are sufficiently comparable.

3. Results

3.1. Evidence Identification, Mapping, and Curated Evidence Base

Electronic database searches identified 15,058 records. After 6226 within- and cross-database duplicates were removed, 8832 unique database-derived records remained. The 73 unique curated references were reconciled separately rather than simply added to the identification count: 41 overlapped the database corpus, and 32 were unique additions. The combined unique corpus therefore contained 8864 records.

Rule-based mapping of the 8832 database-derived records classified 2617 as Core Primary Candidate, 3096 as Contextual Evidence, 1318 as Manual Review, and 1801 as Exclude. These categories accounted for all database-derived records and were retained as automated evidence-mapping strata.

The automated categories did not constitute final full-text inclusion decisions. In particular, a Core Primary Candidate label indicated bibliographic evidence of potential relevance, whereas the final CORE designation required full-text confirmation that a functionally integral micro-/nanoscale feature participated in recognition, analyte–interface interaction, or transduction.

Full-text adjudication of the 73 unique curated records produced 26 CORE primary studies, 17 boundary experimental studies, eight contextual experimental/material studies, 18 review/contextual sources, two methodological sources, and two exclusions. One duplicate source file representing the same study was consolidated before the 73-record count was finalized.

The detailed critical synthesis and reporting-completeness analysis were based on the 26 CORE studies identified within the curated full-text subset. These 26 studies do not constitute an exhaustive set of all potentially eligible studies among the 2617 automated Core Primary Candidate records. Boundary experimental and contextual material studies were retained only for clearly labeled interpretive context and did not contribute to the reporting-completeness frequencies or Table S5 coding.

The CORE set covered electrochemical and impedimetric interfaces; optical, colorimetric, and fiber-optic sensors; quartz-crystal-microbalance gas sensing; and capacitive, resistive, and field-effect-transistor humidity sensors. MEMS/microcantilever reports and several macroscale packaging or gas-sensing studies remained useful contextual evidence but did not enter the strict 26-study synthesis. Figure 2 summarizes the evidence-identification, automated-mapping, reconciliation, and full-text-adjudication workflow.

3.2. Functional Roles and Analytical Taxonomy

Within the 26 CORE studies assessed in the curated subset, the functional roles of chitosan followed the four categories defined in Section 2.7. Individual studies could assign more than one role, and the measured response depended on the complete sensing architecture.

Accordingly, the presence of chitosan was not treated as evidence that sensor performance was chitosan-driven. When selectivity or amplification arose mainly from an aptamer, enzyme, molecular imprint, metal oxide, nanocarbon, nanoparticle, optical probe, patterned electrode, or transistor, performance was attributed to the complete sensing interface rather than to the polymer alone.

Across the assessed curated evidence, the principal interpretive sequence was: fabrication route → micro-/nanostructure → interfacial property → analyte interaction → transducer response. Figure 3 summarizes this role–structure–transduction–evidence relationship.

Material descriptors such as molecular weight and degree of deacetylation were not reported consistently enough to establish transferable cross-study relationships. By contrast, within-study comparisons more often linked film/interface thickness, porosity,

filler distribution, accessible surface area, and transducer geometry to response magnitude, response time, hysteresis, or recovery.

3.3. Fabrication Routes and Micro-/Nanoscale Architectures

3.3.1. Large-Area and Localized Solution Processing

Large-area solution casting was common in the broader contextual literature on optical and freshness-indicator films. These studies remain useful for understanding formulation, dye migration, swelling, and packaging constraints, but macroscale indicator films were not automatically classified as CORE unless a functionally integral micro-/nanoscale architecture was demonstrated.

Within the CORE set, localized drop, dip, and cast deposition were used on microelectrodes, interdigitated electrodes, optical fibers, quartz crystal microbalances, and other miniaturized transducers. Reproducibility depended on deposited volume, wetting, layer number, dry-film thickness, and post-treatment, making incomplete fabrication reporting a direct source of device-to-device uncertainty [8,14,31,51,52,56,59].

Spin coating and related controlled thin-film deposition offered improved thickness control where reported. The chitosan/Au and chitosan/Ag optical waveguide sensor, for example, used an approximately 150 nm film containing sub−10 nm metal nanoparticles [48]. Such measurements provide stronger structural evidence than nominal solution concentration alone.

3.3.2. Patterned and Electrically Directed Deposition

Electrodeposition provided localized control of chitosan-containing interfaces in CORE electrochemical platforms, including molecularly imprinted glyphosate sensors and polypyrrole–chitosan–iron-oxide composites [8,17,23]. Applied potential, deposition time, template composition, and post-treatment were therefore considered part of the sensing architecture rather than incidental processing details.

Printing was represented in the CORE set by the PVA/chitosan/nanocarbon humidity platform coupled to a field-effect transistor [53]. Its amplified output illustrated why printed geometry and transistor gain must be separated from intrinsic film sensitivity. Printed chitosan humidity devices that lacked a functionally integral micro-/nanoscale sensing feature were retained only as boundary evidence.

3.3.3. High-Surface-Area and Hierarchical Interfaces

High-surface-area architectures included electrospun quaternized-chitosan nanofibers [34], a nanofiber-coated QCM with chitosan overlay [59], submicron chitosan particles on ZnO/Pt [82], metal-oxide and nanocarbon electrochemical composites [9,11,14,15,17–23], and plasmonic chitosan nanocomposite films [48]. These architectures increased accessible interface area but also made component-specific attribution more dependent on appropriate controls.

However, hierarchical architectures also complicated functional attribution. Their measured responses resulted from the combined effects of chitosan affinity, nanostructure surface area, porosity, filler hydrophilicity, diffusion pathways, mechanical properties, and transducer amplification. Comparisons with both chitosan-free and nanostructure-free controls were therefore needed to isolate the contribution of each component.

3.3.4. Crosslinking Trade-Offs

Crosslinking improved water resistance, mechanical integrity, and dimensional stability, but it could also restrict polymer-chain mobility and consume or hinder amino groups involved in chelation, proton transport, analyte partitioning, and biomolecule immobilization. The relevant design objective was therefore not maximum crosslink density, but the

minimum degree of crosslinking required to maintain film stability under the intended sample, temperature, and humidity conditions. These trade-offs were particularly relevant to imprinted, fluorescent, ion-binding, and humidity-responsive films [6,13,15,23,30,39,65].

3.4. Electrochemical and Impedimetric Sensors

Within the strict CORE set, electrochemical and impedimetric interfaces addressed glyphosate [8,23], glucose [9,17,82], lactose [11], nitrite [10], cadmium [14], Pb^{2+}/Hg^{2+} [15], 5-fluorouracil [18], paracetamol [19], botulinum neurotoxin A [21], and 4-nitrophenol [22]. Chitosan usually functioned as a film-forming, immobilization, imprinting, analyte-partitioning, or composite-support phase rather than as the principal electrocatalyst. Representative CORE electrochemical and impedimetric sensors are summarized in Table 2.

Table 2. Representative CORE electrochemical and impedimetric sensors with explicitly reported performance.

Architecture	Target	Dominant Chitosan Role	Reported Performance	Critical Interpretation	Ref.
Imprinted chitosan/Au microelectrode	Glyphosate	Recognition matrix	0.31 pg mL^{-1}–50 ng mL^{-1}; LOD 0.001 pg mL^{-1}	Non-imprinted controls isolate imprinting from nonspecific adsorption	[8]
Cu-cysteamine/chitosan electrode	Glucose	Immobilization/binder matrix	2.7 μM–1.3 mM and 1.3–7.7 mM; LOD 0.28 μM	Cu-cysteamine supplies the dominant electrocatalytic response; chitosan immobilizes the active phase	[9]
g-C3N4/magnetic chitosan/enzyme	Lactose	Composite and enzyme support	LOD 0.3 mM; 0.9–100 mM; 5 s; 4.4 μA mM^{-1} *	Enzyme and g-C3N4 dominate recognition/electron transfer; chitosan stabilizes particles and immobilizes enzyme	[11]
AuNP/MWCNT/chitosan aptasensor	Cd^{2+}	Aptamer immobilization matrix	10^{-13}–10^{-4} M; LOD ≈ 2.0×10^{-14} M	Selectivity arises from the aptamer; AuNP/MWCNTs amplify charge transfer	[14]
Chitosan/aptamer MIP–TDNs/AuNPs/MWCNTs/GCE	Pb^{2+} and Hg^{2+}	Recognition and imprinting matrix	LOD 0.0025 μg mL^{-1} Pb^{2+} and 0.0064 μg mL^{-1} Hg^{2+}; seafood validation	Performance arises from the combined MIP/aptamer/nanocarbon architecture	[15]
Cs-Cur-A/NiO nanorods on GCE	5-fluorouracil	Modified chitosan film/composite matrix	0.1–150 μM; LOD 21.75 nM; serum and urine validation	NiO nanorods provide major electrocatalytic contribution; modified chitosan supports the interface	[18]
AuNP/graphene-chitosan immunointerface	Botulinum neurotoxin A	Biocompatible immobilization matrix	0.27–268 pg mL^{-1}; LOD 0.11 pg mL^{-1}; milk/serum validation	Antibody recognition and AuNP/graphene amplification dominate specificity and signal gain	[21]
ZnO/Pt/GCSPs/GOx	Glucose	GOx immobilization/supporting layer	0.05–1 mM; 88.36 μA mM^{-1} cm^{-2}; LOD 0.03 mM; RSD 3.2%	Submicron chitosan supports enzyme loading; Pt/ZnO and GOx govern catalysis and recognition	[82]

* The source article reports 40.8 μA mM^{-1} in its Abstract, whereas its calibration equation, Results section, and Conclusion section report 4.4 μA mM^{-1}; the latter value was used here. AuNP: gold nanoparticle; MWCNT: multi-walled carbon nanotube; MIP: molecularly imprinted polymer; TDN: tetrahedral DNA nanostructure; GCE: glassy carbon electrode; RSD: relative standard deviation.

Evidence supporting a chitosan-specific contribution was strongest when matched controls separated polymer, receptor, filler, and transducer effects. Molecularly imprinted glyphosate devices used non-imprinted controls [8,23]; aptamer and nanocarbon architectures isolated recognition and amplification contributions [14,15]; and composite glucose or drug sensors compared bare, chitosan-containing, and catalytic-material electrodes [9,18,19,21,82].

Several studies that were previously discussed alongside these devices did not remain in the strict CORE set. Chitosan-coated graphite for flubendiamide [12], a chitosan MIP screen-printed p-aminophenol sensor [13], and a polypyrrole-doped chitosan sulfite sensor [20] were retained as boundary evidence because the available full text did not establish a functionally integral micro-/nanoscale feature strongly enough under the final operational definition.

Consequently, limits of detection, sensitivities, and analytical ranges were interpreted as properties of the complete sensing architecture. Claims about an intrinsic chitosan contribution were considered strongest when a control architecture isolated the polymer from receptor activity, catalytic enhancement, nanocarbon conductivity, or transducer gain.

Direct numerical ranking among these devices was not appropriate because they differed in analyte, sample matrix, response mechanism, calibration model, concentration unit, and validation procedure. The more defensible comparison concerned whether each study used appropriate controls to establish the contribution of chitosan.

3.5. Optical, Fluorescent, and Colorimetric Sensors

The strict CORE optical/colorimetric set was narrower than the broader chitosan packaging and fluorescence literature. It included chitosan-coated Mn-doped ZnS micromaterials for ampicillin [25], a chitosan-coated plastic optical fiber for Cd^{2+} [31], electrospun quaternized-chitosan nanofibers used as a pH-responsive freshness interface [34], a CS/PAA fiber-optic Ni^{2+} sensor [42], chitosan/Au and chitosan/Ag optical H_2S waveguides [48], and a micrometer-scale chitosan/Nessler ammonia film [49].

These studies also illustrate different functional roles. Chitosan can provide the analyte-binding or partitioning interface, host an optical or enzymatic element, or form the micro-/nanoscale structure that controls transport to the active probe. Accordingly, fluorescence quenching, plasmonic response, or color generation was not attributed to chitosan when the dominant signal arose from a nanoparticle, pigment, enzyme, or reagent.

Macroscale anthocyanin smart-packaging films [27–29,32,35–37] and several solution-phase fluorescent chitosan derivatives [24,26,30,39] remained useful contextual or boundary evidence, but they were not pooled with CORE sensor performance. Their inclusion as context preserves information on formulation and application while maintaining the stricter micro-/nanosensor boundary requested for the critical synthesis. Representative CORE optical, colorimetric, and fiber-optic sensing interfaces are summarized in Table 3.

Table 3. Representative CORE optical, colorimetric, and fiber-optic chitosan sensing interfaces.

Architecture	Target	Dominant Chitosan Role	Reported Performance	Critical Interpretation	Ref.
Chitosan-coated Mn-doped ZnS + β-lactamase	Ampicillin	Particle/enzyme immobilization matrix	13.1–72.2 pM; LOD 8.24 pM; water and milk matrices	Luminescent particle and enzymatic reaction generate the signal; chitosan supports the interface	[25]
Chitosan-coated plastic optical fiber	Cd^{2+}	Chelating coating/analyte partitioning	Etched core ≈ 498 µm; optical-intensity response and sensitivity/resolution reported	Micro-scale optical transducer is integral; competing-metal and real-water validation were not reported	[31]

Table 3. *Cont.*

Architecture	Target	Dominant Chitosan Role	Reported Performance	Critical Interpretation	Ref.
PVA/PCL/QCS electrospun nanofiber film	pH/beef freshness	Nanofibrous structural and transport interface	Fibers ≈ 100–229 nm; ΔE response; pH 2–12; beef validation	Pigments generate color while nanofiber/QCS architecture controls transport and film behavior	[34]
CS/PAA layer-by-layer no-core fiber	Ni^{2+}	Chelating recognition/partitioning layer	0.05537 nm μM^{-1}; LOD 0.1671 μM; five regeneration cycles	Chitosan/PAA binding layer is separated from the interferometric transducer	[42]
Chitosan/Au and chitosan/Ag waveguide films	H_2S	Nanoparticle host and gas-permeable thin film	≈150 nm film; <10 nm NPs; 0.1–100 ppm Ag and 5–300 ppm Au ranges	Metal-particle sulfidation drives the optical response; RH and gas cross-sensitivity were tested	[48]
Chitosan/Nessler microdiffusion film	Ammonia	Micrometer-scale reagent-support film	15 ± 3 μm film; 28 μg L^{-1}–28 g L^{-1}; serum/artificial urine validation	Nessler reagent provides ammonia-specific color chemistry; chitosan forms the sensing layer	[49]

CS, chitosan; LOD, limit of detection; PAA, poly(acrylic acid); PCL, polycaprolactone; PVA, poly(vinyl alcohol); QCS, quaternized chitosan; RH, relative humidity.

3.6. Gas, Volatile Organic Compound, and Gravimetric Sensors

3.6.1. Chemiresistive, Electrochemical, Optical, and Voltage-Based Gas Responses

Under the final operational definition, most conventional chitosan gas and VOC films were classified as boundary rather than CORE because their available full texts did not establish a functionally integral micro-/nanoscale sensing feature. This applied to chitosan/SnO_2 acetone films [43], electrodeposited hexanal films [44], chitosan/TiO_2 ammonia films [45], cadmium-loaded chitosan for H_2S [46], optical-fiber ammonia coatings without reported micro-/nanoscale coating dimensions [47], and direct chitosan ammonia films [50]. These records remain informative for mechanism and humidity-confounding discussion but do not contribute to CORE performance frequencies.

The strict CORE gas evidence comprised two optical/colorimetric systems and one gravimetric system. Chitosan/Au and chitosan/Ag nanocomposite waveguides detected H_2S using approximately 150 nm chitosan films containing sub−10 nm metal nanoparticles and explicitly examined humidity and gas cross-sensitivity [48]. A chitosan/Nessler film used a 15 ± 3 μm sensing layer for ammonia detection in microdiffusion devices and was validated in serum and artificial urine [49].

These examples reinforce the need to distinguish chitosan's transport or support role from the component that supplies analyte-specific chemistry. In the H_2S waveguide, the metal nanoparticles provide the dominant sulfide-responsive plasmonic change; in the ammonia film, the Nessler reagent supplies the color reaction while chitosan forms the supporting sensing layer.

3.6.2. QCM Gravimetric Sensing

The CORE gravimetric example was a poly(vinyl acetate) nanofiber QCM with a chitosan overlay for ammonia. Adding 0.7 wt% chitosan increased sensitivity from 0.076 to 3.012 Hz ppm^{-1}; the reported LOD was 0.526 ppm, with response and recovery times of 9 and 35 s [59]. The study also tested competing gases, quantified humidity effects, reported repeatability, and followed stability for up to 75 days with an additional three-month storage check.

Microcantilever and MEMS reports [60–62] remain relevant to the broader field and to the device-readiness framework, but they were not part of the final 26-study CORE set after the curated full-text audit. They are therefore treated as contextual examples rather than as contributors to the strict quantitative reporting-completeness results.

3.6.3. Humidity as a Confounder

Humidity is a major confounder in gas and VOC sensing because water adsorption alters chitosan mass, dielectric properties, ionic transport, swelling, and mechanical stress. The QCM ammonia study [59] and the H_2S optical-waveguide study [48] explicitly evaluated humidity effects; this level of control was not consistently present in the boundary gas literature [43–47,50].

A minimum informative protocol should report target-gas response at defined RH, humidity-only response, and, where feasible, mixed gas/RH exposure. Repeated exposure and regeneration should be used to evaluate reversibility, recovery, hysteresis, and drift.

3.6.4. Attribution of the Active Phase

Across gas and gravimetric architectures, chitosan may function as the principal sorption layer, an analyte-partitioning overlay, or a support for a more selective optical or catalytic phase. These configurations were kept analytically distinct rather than grouped under a single generic label of 'chitosan gas sensor'. Representative CORE gas and gravimetric sensing interfaces are summarized in Table 4.

Table 4. Representative CORE gas and gravimetric chitosan sensing interfaces.

Platform	Analyte/RH	Response Metric and Conditions	Dynamics/Stability/ Validation	Attribution Issue	Ref.
Chitosan/Au or chitosan/Ag optical waveguide	H_2S	Plasmonic optical response; room-temperature gas exposure	RH and gas cross-sensitivity evaluated; two-month optical stability	Metal nanoparticle sulfidation dominates the optical signal; chitosan hosts and transports analyte	[48]
Chitosan/Nessler microdiffusion film	Ammonia	Colorimetric ΔRGB response in microdiffusion device	Triplicate measurements; serum and artificial-urine validation	Nessler reagent provides recognition; chitosan is the micrometer-scale support/interface	[49]
PVAc nanofiber + chitosan QCM	NH_3	3.012 Hz ppm^{-1}; LOD 0.526 ppm	9 s/35 s; repeatability, humidity correction, 75-day stability	Response combines chitosan–ammonia interaction with nanofiber surface area and QCM mass loading	[59]

LOD, limit of detection; PVAc, poly(vinyl acetate); QCM, quartz crystal microbalance; RH, relative humidity.

Optical color/intensity response and QCM frequency sensitivity represent different physical quantities and were not combined into a single numerical ranking.

3.7. Humidity Sensors

Humidity sensing provided the clearest CORE examples in which chitosan itself acted as a primary responsive material. Water uptake at amino and hydroxyl groups changes dielectric polarization, polymer swelling, protonic/ionic transport, resistance, and impedance. The same hydration processes can also produce hysteresis, baseline drift, delayed recovery, or structural damage when the exposure protocol is severe [51–56,82].

The six CORE humidity platforms used different transduction and amplification schemes: chitosan–NaCl capacitive sensing [51], flexible capacitive respiratory monitor-

ing [52], a PVA/chitosan/nanocarbon resistor coupled to a field-effect transistor [53], dual capacitive/resistive sensing controlled by electrode geometry [54], a pristine chitosan resistive device for respiration and non-contact skin monitoring [56], and a CS/GO/SnO_2 impedance film [83]. Their reported response magnitudes are therefore not interchangeable measures of intrinsic chitosan sensitivity. Representative CORE humidity-sensing platforms are summarized in Table 5.

Table 5. Representative CORE capacitive, resistive, field-effect-transistor, and impedance humidity sensors.

Architecture	RH Range/Use	Reported Response or Sensitivity	Response/Recovery	Key Limitation	Ref.
CS–50 wt% NaCl film on Pt IDE	6–92% RH	86,492.84% response at ~92% RH; 1017.2 pF/%RH	Composite slower than pure CS; 30 h durability reported	NaCl greatly amplifies dielectric/ionic response but increases hysteresis and slows transport	[51]
Flexible chitosan capacitor	43–97% RH; respiration	35.9 pF/%RH (56–97% RH)	0.7/2 s during breathing; 68/42 s for RH step	Dynamics depend strongly on exposure protocol	[52]
Printed PVA/CS/NCP resistor + FET	33–98% RH	1.74 resistor; 6.27 FET at 98% RH	Low hysteresis; multiple devices and up to 100 repetitions; 15-day stability	FET amplification is not intrinsic material sensitivity	[53]
Dual capacitance/resistance chitosan sensor	6–92% RH	5382.29% capacitance; 99.99% resistance	<10/<30 s; repeated cycles	Electrode geometry changes electric field and ion-transport pathways	[54]
Drop-cast chitosan on Ti/Au IDE	11–95% RH; respiration and non-contact skin monitoring	Average sensitivity 2.58 $M\Omega\%RH^{-1}$; maximum ≈ 5.8 $M\Omega\%RH^{-1}$	21/25 s; maximum hysteresis ≈ 9.3%; 60-day stability	Pristine chitosan is the responsive phase; rigid substrate limits mechanical generalization	[56]
CS/GO/SnO_2 impedance film	15–95% RH	Composite impedance response exceeded CS, CS/GO, and CS/SnO_2 controls	Repeated adsorption/desorption; 30-day stability at 85% RH	GO and SnO_2 add adsorption sites; chitosan remains the hydrophilic matrix	[83]

CS, chitosan; FET, field-effect transistor; GO, graphene oxide; NCP, nanocarbon powder; PVA, poly(vinyl alcohol); RH, relative humidity; SnO_2, tin oxide.

Dynamic performance also depended on the test protocol. The flexible capacitive sensor, for example, responded within approximately 0.7/2 s during breathing but required approximately 68/42 s for a large controlled RH step [52]. This difference illustrates why respiratory-cycle response should not be equated with equilibrium response time under sustained humidity changes.

Boundary humidity studies using chitosan/PEO [57], mealworm-derived CS/PVA [55], printed chitosan films on flexible substrates [58], and related macroscale platforms were retained as supporting context but excluded from strict CORE performance synthesis. This separation reduces the risk of interpreting flexible-device demonstrations or nanoparticle-containing inks as micro-/nanosensors solely because a nanoscale material was present.

Within CORE, reporting was strongest when studies combined defined RH and temperature conditions with structural characterization, repeated cycles, long-term stability, and application demonstrations. Cross-platform comparison nevertheless remains appropriate only when RH protocol, response definition, operating frequency or potential, film/interface geometry, and amplification mechanism are sufficiently comparable.

3.8. Recurrent Reporting Gaps and Evidence Strength

The final reporting-completeness assessment was based exclusively on the 26 CORE studies assessed within the curated full-text subset. Chitosan identity was adequately reported in 17/26 studies (65.4%); fabrication reproducibility in 23/26 (88.5%); film/interface characterization in 23/26 (88.5%); functional-role reporting in 25/26 (96.2%); and response definition in 26/26 (100.0%). Operating conditions were adequate in 21/26 studies (80.8%).

Selectivity/interference testing was reported in 17/26 studies (65.4%), repeatability/reproducibility in 23/26 (88.5%), stability in 13/26 (50.0%), and application validation in 20/26 (76.9%). These frequencies describe reporting completeness within the assessed curated CORE subset and should not be interpreted as prevalence estimates for all potentially eligible studies in the broader evidence map.

These frequencies describe reporting completeness rather than methodological quality or risk of bias. A study could report a well-defined response yet provide limited evidence on long-term stability or interference. Conversely, absence of a reporting criterion does not prove that the underlying device is invalid; it indicates that the corresponding evidence could not be verified from the published full text. Likewise, satisfaction of the functional-role reporting criterion indicates that the stated role of chitosan was distinguished from other device components; it does not necessarily demonstrate a causal contribution experimentally.

The strongest evidence chains linked chitosan identity and formulation to fabrication parameters, measured film/interface structure, functional-role controls, transducer response, operating conditions, selectivity, repeated measurements, stability, and application validation. The recurrent gaps identified by the 26-study matrix therefore support the review's emphasis on reproducibility, causal attribution, realistic validation, and device readiness.

4. Discussion

4.1. A Unified Interpretation of Chitosan Sensor Performance

Within the assessed curated CORE subset, the term "chitosan-based sensor" described material composition but did not by itself identify the causal source of performance. The functional-role categories defined in Section 2.7 were therefore used to distinguish the stated role of chitosan from the contributions of receptors, fillers, catalytic materials, transducer geometry, and amplification mechanisms.

Functional-role reporting was adequate in 25/26 assessed CORE studies (96.2%), but this reporting criterion should not be equated with experimental proof of causality. Causal attribution was stronger when matched controls or controlled comparisons isolated the effect of chitosan. Where such controls were absent, sensitivity, limit of detection, and related performance metrics were interpreted as properties of the complete hybrid interface rather than of chitosan alone.

The same framework explains why a common cross-platform ranking is inappropriate. Current, impedance, optical intensity, wavelength shift, QCM frequency, capacitance, resistance, and FET response are different physical quantities. Even within one transduction class, comparison is defensible only when analyte or RH range, response definition, operating conditions, calibration procedure, and device geometry are sufficiently comparable.

The practical objective is therefore not to identify a universally superior chitosan sensor, but to establish whether the polymer's role is causally supported and whether the complete device has been validated using controls and conditions appropriate to its transduction mechanism.

4.2. Material Identity, Molecular Weight, Degree of Deacetylation, and Chemical Modification

Among the 26 CORE studies assessed within the curated subset, 17/26 (65.4%) met the prespecified chitosan-identity criterion, which required a source plus at least one relevant specification. This incomplete reporting limits interpretation because molecular weight, degree of deacetylation, purity or grade, biological source, and chemical derivatization can all affect solution behavior and sensing-interface properties [2–6].

Molecular weight influences viscosity, chain entanglement, coating uniformity, film cohesion, adhesion, and diffusion. Higher molecular weight can improve mechanical integrity but may increase thickness or aggregation; lower molecular weight may facilitate processing and mass transport while reducing cohesion. The direction of the effect therefore depends on deposition route, thickness, porosity, crosslinking, and transducer geometry.

Degree of deacetylation controls the abundance of protonatable amino groups and can influence chelation, hydrogen bonding, hydration, ionic transport, analyte partitioning, biomolecule immobilization, and crosslinking [3–6]. A higher value may increase available amino groups, but the resulting changes in crystallinity, swelling, nonspecific adsorption, and mechanics make a universal monotonic relationship with sensor performance unlikely.

Chemical modification introduces an additional source of heterogeneity that should not be conflated with unmodified chitosan. The CORE set included, for example, quaternized chitosan in electrospun pH-responsive nanofibers [34] and a chitosan–curcumin Schiff-base matrix combined with NiO nanorods [18]. Such modifications change charge density, solubility, binding chemistry, hydration, and interfacial organization. Their performance should therefore be compared with an appropriate unmodified or equivalent-matrix control before being generalized as a property of chitosan itself.

Future factorial studies should vary molecular weight, degree of deacetylation, modification state, film/interface thickness, and crosslinking independently while controlling concentration, solvent, substrate, filler/receptor loading, environmental conditions, and response definition. Until such data are available, these variables are best treated as essential material descriptors rather than universal design rules.

4.3. Gas–Humidity Discrimination as a Minimum Validity Test

The most consequential platform-specific validity issue remains gas–humidity confounding. Water vapor directly changes chitosan sorption, swelling, proton mobility, dielectric behavior, mass loading, and mechanical stress. Within the strict CORE gas evidence, the QCM ammonia sensor explicitly corrected for humidity and tested competing gases [59], while the chitosan/Au and chitosan/Ag H_2S waveguides evaluated relative-humidity influence and gas cross-sensitivity [48]. This level of control was not consistently present in the broader boundary gas literature [43–47,50].

A gas sensor that performs under dry or narrowly fixed carrier-gas conditions may show baseline shifts, reduced selectivity, slower recovery, or saturation at realistic humidity. Conversely, a humidity-driven change in resistance, capacitance, resonant frequency, optical response, or stress may be misinterpreted as target-gas response when RH is not measured independently.

Gas-sensing studies should therefore report baseline definition, temperature, RH, flow rate where relevant, analyte concentration, exposure duration, response/recovery definitions, regeneration, and drift. At minimum, target-gas exposure at defined RH should be complemented by humidity-only testing; mixed gas/RH experiments are preferable when the intended application is environmental or breath-related.

Quantitative humidity-interference analysis is more informative than qualitative statements of selectivity. Calibration at multiple fixed RH values, comparison of RH-only and analyte responses, and repeated mixed-condition exposure can determine whether

apparent selectivity arises from target-specific chemistry or from the general hydrophilic response of chitosan.

The same controls clarify functional attribution. Chitosan may be the primary sorption-responsive layer, a partitioning coating that concentrates analyte near a transducer, or a support for a more selective nanoparticle, reagent, or catalytic phase. These configurations should not be interpreted as mechanistically equivalent forms of a generic 'chitosan gas sensor'.

4.4. Sustainability and Commercialization Trade-Offs

Chitosan offers several potential sustainability advantages, including renewable sourcing, aqueous processability, chemical versatility, and partial biodegradability [1,3–5,63,69,77]. However, the incorporation of a bio-derived sensing layer does not, by itself, demonstrate that the complete device is biodegradable, environmentally preferable, or compatible with circular-material strategies. Many reported platforms also contain petroleum-derived substrates, poly(vinyl alcohol), polyethylene terephthalate, noble metals, synthetic dyes, metal oxides, carbon nanomaterials, and other persistent electronic or structural components [14,17–22,27–29,32–34,41,53,58,71–76].

Sustainability claims should therefore distinguish among renewable material content, biodegradability of the sensing layer, biodegradability of the complete device, energy and solvent requirements during fabrication, operational lifetime, reusability, toxicity, recyclability, and end-of-life management. The presence of chitosan alone is insufficient evidence of a lower environmental burden. Comparative process-level information or life-cycle assessment is needed to determine whether a chitosan-containing architecture offers a meaningful environmental advantage over an established synthetic polymer or commercial sensing platform.

Commercialization is constrained by several properties that also enable chitosan sensing. Hydrophilicity enhances water-vapor uptake and can improve humidity, gravimetric, and volatile-compound responses, but it may also cause swelling, hysteresis, baseline drift, delayed recovery, and loss of dimensional stability. Chemical reactivity facilitates receptor immobilization, crosslinking, and composite formation, but may increase sensitivity to formulation conditions and batch-to-batch variation. Biodegradability may reduce material persistence after disposal, but it can conflict with shelf life, storage stability, sterilization, packaging requirements, and long-term operation.

These trade-offs indicate that complete biodegradability should not necessarily be treated as the only or most appropriate design objective. A more practical architecture may separate disposable or degradable sensing components from durable electronic components, an approach consistent with broader developments in biodegradable and transient electronics [78]. For chitosan-based sensors, for example, a replaceable sensing element could be integrated with a reusable electronic reader, optical interrogation unit, or resonant transducer [1,58,79]. Such a modular design could reduce material consumption while preserving calibration stability, signal-processing capability, and device reliability.

Commercial readiness also requires attention to raw-material consistency, manufacturing tolerance, coating uniformity, storage conditions, quality control, cost, and regulatory or safety requirements. Chitosan source, molecular weight, degree of deacetylation, purity, and residual contaminants may vary among suppliers and production batches, potentially affecting film formation and sensing performance. Scalable manufacturing therefore requires material specifications and process controls that are more rigorous than those typically reported in proof-of-concept studies.

Overall, defensible sustainability and commercialization claims should be based on the complete sensing system rather than on the origin of a single material component. The

most credible development pathway is likely to combine renewable or replaceable chitosan sensing layers with durable, reusable readout components, standardized fabrication, demonstrated operational stability, and an explicit end-of-life strategy. This framing is consistent with the manuscript's broader distinction between material-level promise and device-level readiness.

4.5. Device-Readiness Pathway and Actionable Research Agenda

The assessed curated evidence was dominated by material demonstrations and proof-of-concept sensors. To distinguish exploratory studies from devices approaching practical deployment, this review proposes a four-stage device-readiness pathway comprising material proof of concept, validated prototype, application validation, and deployable system. Progression through these stages requires increasingly rigorous evidence concerning material identity, fabrication reproducibility, analytical validity, performance under realistic operating conditions, and system-level feasibility. This distinction is particularly important because much of the evidence assessed in the curated subset remains at the proof-of-concept or early-prototype stage [8–62]. Figure 4 summarizes the four-stage pathway and the evidence gates required for progression.

At the material proof-of-concept stage, a study should establish whether the proposed chitosan film or interface produces a measurable response that is consistent with the intended sensing mechanism. Minimum material reporting should include the chitosan source or commercial grade, molecular weight, degree of deacetylation, concentration, solvent composition, solution pH, derivative or crosslinker, filler type and loading, and any receptor or recognition element. Fabrication reporting should include the deposition method, process parameters, substrate, drying or post-treatment conditions, film thickness, morphology, and transducer geometry. Initial sensitivity, selectivity, or response behavior may be demonstrated at this stage, but conclusions should remain limited to technical feasibility and should not imply application or commercial readiness.

A validated prototype should demonstrate that the observed response is analytically interpretable, reproducible, and attributable to the proposed sensing architecture. Studies should provide an explicit response equation, baseline definition, calibration range, sensitivity, limit of detection and limit of quantification where analytically meaningful, response and recovery times, selectivity, repeatability, hysteresis, baseline drift, and operational or storage stability. The number of independently fabricated devices and material batches should also be reported. Appropriate controls should distinguish the contribution of chitosan from those of fillers, receptors, nanostructures, additives, electrode geometry, and transducer amplification. Depending on the architecture, relevant controls may include chitosan-free, filler-free, receptor-free, non-imprinted, or equivalent-matrix devices.

Application validation requires testing under realistic sample matrices or exposure conditions rather than exclusively under idealized laboratory conditions. The required validation should be matched to the transduction mechanism, analyte, sample matrix, environmental conditions, and intended use. Such validation should determine whether calibration, selectivity, response dynamics, and stability are retained when the device is exposed to realistic interferents, temperature and humidity variations, mechanical deformation, complex matrices, or prolonged operation.

A deployable system requires evidence beyond analytical performance. Relevant requirements include defined manufacturing tolerances, quality-control criteria, batch consistency, shelf life, packaging stability, calibration transfer, safety, cost, power consumption, signal processing, data interpretation, and a regeneration or replacement strategy. Integration with readout electronics, optical interrogation systems, wireless communication, smartphone interfaces, or Internet-of-Things platforms may also become relevant at this

stage. Application-specific regulatory requirements should be considered where the device is intended for food monitoring, environmental analysis, clinical use, wearable operation, or direct contact with biological materials.

Sustainability assessment should also become more comprehensive as the device progresses toward deployment. Claims should address the complete sensing system rather than only the bio-derived origin of the chitosan layer. Relevant considerations include material sourcing, solvent and energy requirements, reusable and disposable components, operational lifetime, recyclability, biodegradability, and end-of-life management. A replaceable chitosan sensing layer integrated with a reusable electronic, optical, or resonant reader may provide a more realistic balance among sustainability, reliability, and cost than attempting to make the entire sensing system biodegradable.

The proposed pathway is not intended as a formal regulatory classification or universal technology-readiness scale. Instead, it provides a structured framework for distinguishing material feasibility from analytical validation, realistic application testing, and system-level deployment.

Because the transduction domains measure different physical quantities, a numerical league table or common radar chart would imply a degree of comparability that is not supported by the evidence. Electrochemical current, impedance, capacitance, resistance, resonant-frequency shift, fluorescence intensity, absorbance, color difference, transistor response, and mechanical deflection represent fundamentally different outputs. Figure 5 therefore presents a cross-platform validation matrix rather than a numerical ranking. Each platform is linked to the quantity measured, the typical functional role of chitosan, the principal confounding variables, and the minimum validation required to support a defensible performance claim.

Electrochemical and impedimetric systems should be evaluated in relevant biological, food, pharmaceutical, or environmental matrices and should report analytical recovery, matrix effects, and interference from coexisting species [12,15,16,18–22,66,67]. Optical and colorimetric freshness indicators should be correlated with independent spoilage markers, such as pH, total volatile basic nitrogen, microbial count, or another validated reference measurement [27–29,32–37,71–76]. Gas and volatile-organic-compound sensors should be tested under controlled and variable relative humidity, mixed-gas conditions, and repeated exposure–regeneration cycles [43–50,59]. Wearable humidity sensors should be assessed during repeated bending or deformation, temperature variation, skin-adjacent operation, perspiration exposure, and prolonged cycling [52,53,55–58]. Gravimetric and resonant platforms should additionally report film mass or thickness, resonator characteristics, viscoelastic effects, humidity interference, and repeated sorption–desorption behavior.

The next research priority should therefore not be another isolated record detection limit obtained from a unique hybrid formulation. Greater scientific value would be provided by controlled comparative studies that identify which material, structural, or transducer variable is responsible for improved performance. Priority areas include reference chitosan materials with specified molecular weight and degree of deacetylation, factorial studies of film composition and architecture, standardized film-thickness measurements, interlaboratory fabrication studies, harmonized response definitions, and application-specific validation benchmarks.

Controlled experiments should vary one factor at a time or use statistically designed factorial approaches while maintaining comparable substrates, device geometries, filler concentrations, receptor loadings, film thicknesses, and operating conditions. These studies should report both successful and unsuccessful formulations because selective reporting of the best-performing composition can obscure the actual relationship between formulation

and performance. Device-to-device and batch-to-batch variability should be treated as central outcomes rather than secondary technical details.

Benchmarking requirements should remain specific to each sensing platform. Gas-sensor studies should include humidity discrimination, mixed-gas interference, response reversibility, regeneration, and baseline drift. Optical and colorimetric indicators should include photostability, objective spectral or color calibration, illumination dependence, dye migration, reversibility where applicable, and correlation with an independent analytical method. Wearable humidity sensors should include repeated deformation, temperature interference, skin-adjacent operation, perspiration exposure, long-term drift, and device-to-device reproducibility. Electrochemical and impedimetric interfaces should include controls that isolate the respective effects of chitosan, recognition elements, conductive fillers, and electrode architecture. Gravimetric and resonant systems should report film loading, resonator properties, viscoelastic effects, environmental interference, and repeated sorption–desorption cycles.

Table 6 consolidates these requirements into a proposed minimum reporting standard for future chitosan-film sensor studies. The framework is intended to improve reproducibility, causal attribution, within-platform comparison, and progression from material demonstration to application-ready sensing systems. The reporting categories should not be interpreted as a rigid checklist applicable in identical form to every platform. Rather, each study should report all parameters that are materially relevant to its sensing mechanism, fabrication route, transduction method, and intended application.

Table 6. Proposed minimum reporting standard for future chitosan-film sensor studies.

Category	Minimum Information Required
Chitosan identity	Source, commercial grade or purity, molecular weight, degree of deacetylation, concentration, derivative, and crosslinking conditions
Solution formulation	Solvent composition, pH, additives, receptor concentration, filler type and loading, and solution viscosity where relevant
Fabrication	Deposition method, process parameters, substrate preparation, drying or post-treatment conditions, and number of independently prepared batches
Film or interface	Dry-film thickness, morphology, porosity or roughness, adhesion, active area, filler distribution, and swelling behavior where relevant
Device configuration	Substrate, electrode or transducer geometry, resonator characteristics, operating frequency or potential, readout configuration, and amplification mechanism
Test conditions	Analyte concentration, sample matrix, temperature, relative humidity, flow rate where relevant, equilibration time, exposure duration, and regeneration procedure
Analytical response	Explicit response equation, baseline definition, calibration range, sensitivity, LOD or LOQ where meaningful, and response and recovery definitions
Validity controls	Chitosan-free, filler-free, receptor-free, non-imprinted, or equivalent-matrix controls, together with interference and environmental-control experiments
Reproducibility	Number of devices, repeated cycles, device-to-device variation, batch-to-batch variation, and appropriate statistical reporting
Stability	Baseline drift, operational stability, storage stability, shelf life, mechanical durability, and regeneration performance
Application validation	Real or realistically simulated samples, analytical recovery or reference-method comparison, matrix effects, and application-specific operating conditions
Translation	Manufacturing tolerance, quality control, calibration transfer, power and readout requirements, cost, packaging, safety, and regulatory considerations
Sustainability	Complete-device material inventory, material sourcing, solvent and energy use, reusable and disposable components, lifetime, recyclability, and end-of-life strategy

4.6. Limitations of This Review

This review has several methodological and evidence-base limitations. First, the large-scale evidence map relied on rule-based automated classification of titles, abstracts, keywords, document types, and bibliographic metadata. The resulting classifications were retained without manual modification and were not validated against an independently screened human reference set. Records with missing abstracts, incomplete metadata, uncommon terminology, or ambiguous descriptions may therefore have been misclassified. The four automated categories should consequently be interpreted as reproducible bibliographic classifications rather than definitive study-level eligibility or quality judgments.

Second, the 1318 records classified as Manual Review did not undergo subsequent manual adjudication. Some potentially relevant studies may therefore have remained unresolved. Conversely, some records classified as Core Primary Candidate or Contextual Evidence might not have met all eligibility criteria following full-text assessment. Automated exclusion may also have produced false-negative classifications. The 1801 Exclude records were counted as excluded during automated title and abstract screening, but this classification was not independently verified through duplicate human screening.

Third, the detailed critical synthesis was based on full-text adjudication of a curated subset of 73 records rather than exhaustive full-text assessment of all 2617 automated Core Primary Candidate records. Within this curated subset, 26 studies met the strict CORE criteria, while 17 were classified as boundary experimental studies and eight as contextual experimental/material studies. Accordingly, the 26 CORE studies represent the studies meeting the strict eligibility criteria within the curated subset and should not be interpreted as the complete set of all potentially eligible studies in the broader automated evidence map. This improves scope transparency but does not eliminate selection effects associated with article accessibility, prior identification, supplementary searching, or the composition of the curated library.

Fourth, the primary literature was highly heterogeneous in analytes, sample matrices, chitosan characteristics, film architectures, fabrication methods, transduction mechanisms, device geometries, response definitions, units, operating conditions, and validation procedures. This heterogeneity prevented quantitative meta-analysis and limited direct numerical comparison among studies. Consequently, the review emphasized mechanistic interpretation, within-platform comparison, reporting completeness, and device-readiness considerations rather than pooled performance estimates or cross-platform rankings.

Fifth, the review was restricted to English-language records retrieved from Scopus, PubMed, and IEEE Xplore, supplemented by citation tracking and publisher-platform searching. Studies indexed exclusively in other bibliographic databases, reported in other languages, or available only through poorly indexed conference proceedings, theses, patents, or institutional repositories may therefore have been missed. Database coverage may also have differed across electrochemical, optical, gas, humidity, gravimetric, MEMS, and nanotechnology research communities.

Sixth, the reporting-completeness assessment was descriptive and domain-based, not a validated risk-of-bias instrument. The ten-domain matrix was completed for all 26 CORE studies assessed within the curated subset and is reported as frequencies and percentages, but no composite quality score or certainty-of-evidence rating was assigned. These frequencies describe reporting completeness within the assessed curated subset and should not be interpreted as prevalence estimates for all potentially eligible studies in the broader evidence map. The results should therefore be interpreted as auditable indicators of reporting and validation gaps, not as proof that individual studies are methodologically invalid.

Finally, the review protocol was registered retrospectively, and several refinements—including broader terminology related to MEMS, resonators, microcantilevers, gravimetric

platforms, and nanosensors—were introduced during the review. Although these refinements improved the coverage of heterogeneous sensor architectures, they may have increased the influence of reviewer judgment on the final analytical scope. The functional-role framework, cross-platform validation matrix, minimum reporting standard, and device-readiness pathway should therefore be regarded as structured interpretive and research-guidance tools derived from the assessed curated evidence, rather than as statistically validated scoring systems, exhaustive representations of the broader literature, or formal regulatory classifications.

5. Conclusions

This systematic evidence map and curated critical review indicates that chitosan can perform functionally important roles in micro-/nanoscale sensing interfaces, with its contribution depending on architecture and transduction mechanism. The detailed qualitative assessment was conducted on a curated full-text subset of 73 records, within which 26 studies met the strict CORE criteria. These 26 studies should not be interpreted as the complete set of all eligible studies within the broader automated evidence map.

Within the 26 CORE studies assessed in this curated subset, response definition was reported in 100.0% and functional-role reporting in 96.2%, whereas stability was assessed in 50.0%. Chitosan identity and selectivity/interference each met the reporting criterion in 65.4% of studies. These frequencies describe the assessed subset and are not prevalence estimates for the broader candidate literature.

Among the assessed studies, analytical performance in hybrid electrochemical, optical, and composite devices generally reflected the complete sensing architecture, including receptors, enzymes, metal oxides, nanocarbons, nanoparticles, optical reagents, patterned electrodes, and amplification mechanisms. Functional-role reporting should therefore be distinguished from experimental demonstration of the causal contribution of chitosan. Gas/VOC studies additionally require explicit discrimination between target response and humidity effects, while humidity sensors require standardized RH protocols, dynamic definitions, and long-term testing.

For the assessed evidence set, progression toward more deployable devices requires complete material identity, reproducible fabrication, measured film/interface structure, appropriate component controls, realistic interference testing, device-to-device reproducibility, and stability under intended operating conditions. The role–structure–transduction–evidence framework and device-readiness pathway should therefore be interpreted as structured analytical and research-guidance tools derived from the curated evidence assessed here, rather than as a comprehensive characterization of all potentially eligible studies in the broader literature.

Supplementary Materials: The following supporting information can be downloaded at: https://www.mdpi.com/article/10.3390/micro6040076/s1, Table S1, database-specific search strategies and search metadata; Table S2A–C, identification and deduplication flow, database-origin overlap, and curated-library reconciliation; Table S3, rule-based automated evidence-mapping summary and record-level map; Table S4, final 73-record curated inventory; Table S5, 26-study extraction matrix and reporting-completeness domain summary.

Author Contributions: Conceptualization, M.R. and W.N.; methodology, M.R., A.A., K.P. and W.N.; investigation and data curation, M.R. and A.A.; formal analysis, M.R., K.P. and W.N.; visualization, M.R.; writing—original draft preparation, M.R.; writing—review and editing, A.A., K.P. and W.N.; supervision, W.N. All authors have read and agreed to the published version of the manuscript.

Funding: This research received no external funding.

Data Availability Statement: The bibliographic data supporting this review were derived from the published sources cited in the manuscript. The review protocol is available through the Open Science Framework Registries at DOI: 10.17605/OSF.IO/YDUK9. Database-specific search strategies, deduplication summaries, automated classifications, the final 73-record adjudication inventory, and the 26-study extraction matrix with evidence-line provenance are provided in the Supplementary Materials and associated OSF project.

Acknowledgments: During preparation of this manuscript, the authors used the Google Gemini web application, including Gemini 3.5 and Gemini 3.6 Reasoning, for the purposes of AI-assisted graphical refinement and the addition of scientific illustrative elements to Figures 1–5. The authors have reviewed and edited the output and take full responsibility for the content of this publication.

Conflicts of Interest: The authors declare no conflicts of interest.

References

1. Teixeira, S.C.; Gomes, N.O.; de Oliveira, T.V.; Fortes-Da-Silva, P.; Soares, N.F.F.; Raymundo-Pereira, P.A. Review and perspectives of sustainable, biodegradable, eco-friendly and flexible electronic devices and (bio)sensors. *Biosens. Bioelectron. X* **2023**, *14*, 100371. [CrossRef]
2. Zhang, W.; Cao, J.; Jiang, W. Analysis of film-forming properties of chitosan with different molecular weights and its adhesion properties with different postharvest fruit surfaces. *Food Chem.* **2022**, *395*, 133605. [CrossRef] [PubMed]
3. Cheung, R.C.F.; Ng, T.B.; Wong, J.H.; Chan, W.Y. Chitosan: An update on potential biomedical and pharmaceutical applications. *Mar. Drugs* **2015**, *13*, 5156–5186. [CrossRef] [PubMed]
4. Morin-Crini, N.; Lichtfouse, E.; Torri, G.; Crini, G. Applications of chitosan in food, pharmaceuticals, medicine, cosmetics, agriculture, textiles, pulp and paper, biotechnology, and environmental chemistry. *Environ. Chem. Lett.* **2019**, *17*, 1667–1692. [CrossRef]
5. Muxika, A.; Etxabide, A.; Uranga, J.; Guerrero, P.; de la Caba, K. Chitosan as a bioactive polymer: Processing, properties and applications. *Int. J. Biol. Macromol.* **2017**, *105*, 1358–1368. [CrossRef] [PubMed]
6. Carrera, C.; Bengoechea, C.; Carrillo, F.; Calero, N. Effect of deacetylation degree and molecular weight on surface properties of chitosan obtained from biowastes. *Food Hydrocoll.* **2023**, *137*, 108383. [CrossRef]
7. Annu; Raja, A.N. Recent development in chitosan-based electrochemical sensors and its sensing application. *Int. J. Biol. Macromol.* **2020**, *164*, 4231–4244. [CrossRef] [PubMed]
8. Zouaoui, F.; Bourouina-Bacha, S.; Bourouina, M.; Abroa-Nemeir, I.; Ben Halima, H.; Gallardo-Gonzalez, J.; El Alami El Hassani, N.; Alcacer, A.; Bausells, J.; Jaffrezic-Renault, N.; et al. Electrochemical impedance spectroscopy determination of glyphosate using a molecularly imprinted chitosan. *Sens. Actuators B Chem.* **2020**, *309*, 127753. [CrossRef]
9. Chen, H.; Gu, T.; Lv, L.; Chen, X.; Lu, Q.; Kotb, A.; Chen, W. A Biocompatible, Highly Sensitive, and Non-Enzymatic Glucose Electrochemical Sensor Based on a Copper-Cysteamine (Cu-Cy)/Chitosan-Modified Electrode. *Nanomaterials* **2024**, *14*, 1430. [CrossRef] [PubMed]
10. Al-Kadhi, N.S.; Hefnawy, M.A.; S. Nafee, S.; Alamro, F.S.; Pashameah, R.A.; Ahmed, H.A.; Medany, S.S. Zinc Nanocomposite Supported Chitosan for Nitrite Sensing and Hydrogen Evolution Applications. *Polymers* **2023**, *15*, 2357. [CrossRef] [PubMed]
11. Nasiri, H.; Baghban, H.; Teimuri-Mofrad, R.; Mokhtarzadeh, A. Graphitic carbon nitride/magnetic chitosan composite for rapid electrochemical detection of lactose. *Int. Dairy J.* **2023**, *136*, 105489. [CrossRef]
12. Aghris, S.; Azriouil, M.; Matrouf, M.; Ettadili, F.E.; Laghrib, F.; Saqrane, S.; Farahi, A.; Bakasse, M.; Lahrich, S.; El Mhammedi, M.A. Chitosan biopolymer coated graphite electrode as a robust electrochemical platform for the detection of the insecticide flubendiamide. *J. Food Compos. Anal.* **2022**, *114*, 104749. [CrossRef]
13. Mulyasuryani, A.; Prananto, Y.P.; Fardiyah, Q.; Widwiastuti, H.; Darjito, D. Application of Chitosan-Based Molecularly Imprinted Polymer in Development of Electrochemical Sensor for p-Aminophenol Determination. *Polymers* **2023**, *15*, 1818. [CrossRef] [PubMed]
14. Rabai, S.; Teniou, A.; Catanante, G.; Benounis, M.; Marty, J.L.; Rhouati, A. Fabrication of AuNPs/MWCNTS/chitosan nanocomposite for the electrochemical aptasensing of cadmium in water. *Sensors* **2022**, *22*, 105. [CrossRef] [PubMed]
15. Hao, L.; Zhu, N.; Sha, J.; Fang, X.; Cao, H.; Ye, T.; Yuan, M.; Gu, H.; Xu, F. A novel pH-stable chitosan/aptamer imprinted polymers modified electrochemical biosensor for simultaneous detection of Pb^{2+} and Hg^{2+}. *J. Food Compos. Anal.* **2025**, *144*, 107777. [CrossRef]
16. Krishnan, V.; Pandey, G.R.; Babu, K.A.; Paramasivam, S.; Kumar, S.S.; Balasubramanian, S.; Ravichandiran, V.; Pazhani, G.P.; Veerapandian, M. Chitosan grafted butein: A metal-free transducer for electrochemical genosensing of exosomal CD24. *Carbohydr. Polym.* **2021**, *269*, 118333. [CrossRef]

17. Abdul Amir AL-Mokaram, A.M.A.; Yahya, R.; Abdi, M.M.; Muhammad Ekramul Mahmud, H.N. One-step electrochemical deposition of Polypyrrole–Chitosan–Iron oxide nanocomposite films for non-enzymatic glucose biosensor. *Mater. Lett.* **2016**, *183*, 90–93. [CrossRef]
18. Abd-Elsabour, M.; Abou-Krisha, M.M.; Abdel-Haleem, F.M.; Goda, M.N.; Mohy-Eldin, M.S. Electrochemical Nanomolar Determination of the Anticancer Drug 5-Fluorouracil Using Chitosan Curcumin Schiff Base-Decorated NiO Nanorods Synthesized with Green Method. *J. Electrochem. Soc.* **2024**, *171*, 87520. [CrossRef]
19. Akhter, S.; Basirun, W.J.; Alias, Y.; Johan, M.R.; Bagheri, S.; Shalauddin, M.; Ladan, M.; Anuar, N.S. Enhanced amperometric detection of paracetamol by immobilized cobalt ion on functionalized MWCNTs—Chitosan thin film. *Anal. Biochem.* **2018**, *551*, 29–36. [CrossRef] [PubMed]
20. Adeosun, W.A.; Asiri, A.M.; Marwani, H.M. Fabrication of Conductive Polypyrrole Doped Chitosan Thin Film for Sensitive Detection of Sulfite in Real Food and Biological Samples. *Electroanalysis* **2020**, *32*, 1725–1736. [CrossRef]
21. Afkhami, A.; Hashemi, P.; Bagheri, H.; Salimian, J.; Ahmadi, A.; Madrakian, T. Impedimetric immunosensor for the label-free and direct detection of botulinum neurotoxin serotype A using Au nanoparticles/graphene-chitosan composite. *Biosens. Bioelectron.* **2017**, *93*, 124–131. [CrossRef] [PubMed]
22. Khan, S.B.; Ali, F.; Akhtar, K. Chitosan nanocomposite fibers supported copper nanoparticles based perceptive sensor and active catalyst for nitrophenol in real water. *Carbohydr. Polym.* **2019**, *207*, 650–662. [CrossRef] [PubMed]
23. Zouaoui, F.; Bourouina-Bacha, S.; Bourouina, M.; Alcacer, A.; Bausells, J.; Jaffrezic-Renault, N.; Zine, N.; Errachid, A. Electrochemical Impedance Spectroscopy Microsensor Based on Molecularly Imprinted Chitosan Film Grafted on a 4-Aminophenylacetic Acid (CMA) Modified Gold Electrode, for the Sensitive Detection of Glyphosate. *Front. Chem.* **2021**, *9*, 621057. [CrossRef] [PubMed]
24. Liu, Y.L.; Wang, Z.K.; Qin, W.; Hu, Q.L.; Tang, B.Z. Fluorescent detection of Cu^{2+} by chitosan-based AIE bioconjugate. *Chin. J. Polym. Sci. (Engl. Ed.)* **2017**, *35*, 365–371. [CrossRef]
25. Nguyen, S.H.; Nguyen, V.N.; Tran, M.T. Dual-channel fluorescent sensors based on chitosan-coated Mn-doped ZnS micromaterials to detect ampicillin. *Sci. Rep.* **2024**, *14*, 10066. [CrossRef] [PubMed]
26. Cui, F.; Du, G.; You, K.; Cui, Q.; Chen, L.; Deng, Q.; Li, J. Design of chitosan-based fluorescence sensor for the effective detection of nitroaromatics in 100% aqueous medium and mechanism study. *J. Photochem. Photobiol. A Chem.* **2026**, *478*, 117236. [CrossRef]
27. Merz, B.; Capello, C.; Leandro, G.C.; Moritz, D.E.; Monteiro, A.R.; Valencia, G.A. A novel colorimetric indicator film based on chitosan, polyvinyl alcohol and anthocyanins from jambolan (*Syzygium cumini*) fruit for monitoring shrimp freshness. *Int. J. Biol. Macromol.* **2020**, *153*, 625–632. [CrossRef] [PubMed]
28. Li, B.; Bao, Y.; Li, J.; Bi, J.; Chen, Q.; Cui, H.; Wang, Y.; Tian, J.; Shu, C.; Wang, Y.; et al. A sub-freshness monitoring chitosan/starch-based colorimetric film for improving color recognition accuracy via controlling the pH value of the film-forming solution. *Food Chem.* **2022**, *388*, 132975. [CrossRef] [PubMed]
29. Qin, Y.; Wang, Y.; Tang, Z.; Chen, K.; Wang, Z.; Cheng, G.; Chi, H.; Soteyome, T. A pH-sensitive film based on chitosan/gelatin and anthocyanin from Zingiber striolatum Diels for monitoring fish freshness. *Food Chem. X* **2024**, *23*, 101639. [CrossRef] [PubMed]
30. Meng, Z.; Wang, Z.; Liang, Y.; Zhou, G.; Li, X.; Xu, X.; Yang, Y.; Wang, S. A naphthalimide functionalized chitosan-based fluorescent probe for specific detection and efficient adsorption of Cu^{2+}. *Int. J. Biol. Macromol.* **2023**, *239*, 124261. [CrossRef] [PubMed]
31. Khoiro, M.; Dzulkiflih; Firdaus, R.A.; Rahmawati, E.; Yantidewi, M.; Fadhilah, N.; Khairunnisa, S.A.; Fauziyah, N.A. Sensitive cadmium detection using chitosan-coated plastic optical fiber. *Next Mater.* **2025**, *9*, 101245. [CrossRef]
32. Hidayaty, A.N.; Fiddaroini, S.; Fahmi, A.L.; Siahaan, S.R.A.; Fardiyah, Q.; Srihardyastutie, A.; Sabarudin, A. Chitosan–PVA composite films incorporated with roselle anthocyanins: Colorimetric smart sensor for real-time monitoring of meat and seafood freshness. *Food Chem. X* **2026**, *33*, 103545. [CrossRef] [PubMed]
33. Dong, S.; Zhang, Y.; Lu, D.; Gao, W.; Zhao, Q.; Shi, X. Multifunctional intelligent film integrated with purple sweet potato anthocyanin and quercetin-loaded chitosan nanoparticles for monitoring and maintaining freshness of shrimp. *Food Packag. Shelf Life* **2023**, *35*, 101022. [CrossRef]
34. Zou, X.; Zou, Y.; Zhang, K.; Hashim, S.B.; Xu, H.; Kang, M.; Wu, Y.; Zhang, J.; Huang, X.; Shi, J.; et al. Shikonin and curcumin-incorporated PVA/PCL/quaternized chitosan electrospun nanofiber films with pH-responsive properties for smart/active food packaging. *Food Control* **2027**, *191*, 112422. [CrossRef]
35. Roichatuttamamah, W.; Mahatmanti, F.W.; Kusuma, S.B.W.; Rahayu, E.F. Chitosan/Anthocyanin-Based Indicator Film with Carnauba Wax Addition for Monitoring Chicken Freshness. *J. Kim. Sains Dan Apl.* **2025**, *28*, 283–291. [CrossRef]
36. Tavassoli, M.; Khezerlou, A.; Firoozy, S.; Ehsani, A.; Punia Bangar, S. Chitosan-based film incorporated with anthocyanins of red poppy (*Papaver rhoeas* L.) as a colorimetric sensor for the detection of shrimp freshness. *Int. J. Food Sci. Technol.* **2023**, *58*, 3050–3057. [CrossRef]
37. Zeng, F.; Ye, Y.; Liu, J.; Fei, P. Intelligent pH indicator composite film based on pectin/chitosan incorporated with black rice anthocyanins for meat freshness monitoring. *Food Chem. X* **2023**, *17*, 100531. [CrossRef] [PubMed]

38. Azmi, N.A.; Low, S.C. Investigating film structure of membrane-based colorimetric sensor for heavy metal detection. *J. Water Process Eng.* **2017**, *15*, 37–42. [CrossRef]
39. Pournaki, M.; Fallah, A.; Gülcan, H.O.; Gazi, M. A novel chitosan-based fluorescence chemosensor for selective detection of Fe^{3+} ion in acetic aqueous medium. *Mater. Technol.* **2021**, *36*, 91–96. [CrossRef]
40. Wang, S.; Zheng, M. In situ synthesis of chitosan-capped CuS nanoparticles film as an environmentally friendly fluorescence sensor for phenolic. *Mater. Technol.* **2017**, *32*, 186–190. [CrossRef]
41. Jaiswal, A.; Ghosh, S.S.; Chattopadhyay, A. Quantum Dot Impregnated-Chitosan Film for Heavy Metal Ion Sensing and Removal. *Langmuir* **2012**, *28*, 15687–15696. [CrossRef] [PubMed]
42. Raghunandhan, R.; Chen, L.H.; Long, H.Y.; Leam, L.L.; So, P.L.; Ning, X.; Chan, C.C. Chitosan/PAA-based fiber-optic interferometric sensor for heavy metal ions detection. *Sens. Actuators B Chem.* **2016**, *233*, 31–38. [CrossRef]
43. Nasution, T.I.; Lubis, N.S. Enhancement of the Sensing Properties of Chitosan Films as an Acetone Gas Sensor with the Addition of Tin Oxide (SnO_2). *J. Technomater. Phys.* **2024**, *6*, 69–78. [CrossRef]
44. Shantini, D.; Nainggolan, I.; Nasution, T.I.; Derman, M.N.; Mustaffa, R.; Abd Wahab, N.Z. Hexanal Gas Detection Using Chitosan Biopolymer as Sensing Material at Room Temperature. *J. Sens.* **2016**, *2016*, 8539169. [CrossRef]
45. Nainggolan, I.; Wadana, W.T.; Nasution, T.I.; Sembiring, A. The sensitivity of chitosan/TiO_2 film on ammonia detection. *Mater. Today Proc.* 2024, *in press*. [CrossRef]
46. Aboushouk, M.I.; El-Zomrawy, A.A.; Salem, A.M. Electrochemical Detection of H_2S Gas Based on Chitosan Extracted From Shrimp Shells Loaded Cadmium Ions. *Egypt. J. Chem.* **2022**, *65*, 185–192. [CrossRef]
47. Sidiroglou, F.; Nguyen, T. Synthesis of chitosan films on optical fibers for detection of ammonia vapors. In Proceedings of the 2011 International Quantum Electronics Conference (IQEC) and Conference on Lasers and Electro-Optics (CLEO) Pacific Rim Incorporating the Australasian Conference on Optics, Lasers and Spectroscopy and the Australian Conference on Optical Fibre Technology, Sydney, Australia, 28 August–1 September 2011; pp. 1742–1744. [CrossRef]
48. Mironenko, A.; Sergeev, A.A.; Nazirov, A.E.; Modin, E.B.; Voznesenskiy, S.S.; Bratskaya, S. H_2S optical waveguide gas sensors based on chitosan/Au and chitosan/Ag nanocomposites. *Sens. Actuators B Chem.* **2016**, *225*, 348–353. [CrossRef]
49. Tagliaro, I.; Musile, G.; Caricato, P.; Dorizzi, R.M.; Tagliaro, F.; Antonini, C. Chitosan Film Sensor for Ammonia Detection in Microdiffusion Analytical Devices. *Polymers* **2023**, *15*, 4238. [CrossRef] [PubMed]
50. Chandrasakaran, D.S.; Nainggolan, I.; Ikhsan, T.; Derman, M.N. Ammonia gas sensor based on chitosan biopolymer. *Mater. Sci. Forum* **2015**, *819*, 429–434. [CrossRef]
51. He, A.; Yan, H.; Zheng, G.; Zhou, R.; Li, Y.; Ye, Z.; Zhang, C. A high-sensitive capacitive humidity sensor based on chitosan-sodium chloride composite material. *Colloids Surf. A Physicochem. Eng. Asp.* **2024**, *699*, 134740. [CrossRef]
52. Pan, M.; Zhou, J.; Weng, S.; Wu, X. Flexible Chitosan-Based Capacitive Humidity Sensors for Respiratory Monitoring. *Sensors* **2024**, *24*, 1352. [CrossRef] [PubMed]
53. Liu, R.; Wu, Z.; Li, Q.; Shamim, S.; Ba, L. Fully printed field-effect transistor humidity sensor with chitosan/polyvinyl alcohol/nano carbon powder for enhanced moisture sensitivity. *Talanta* **2025**, *287*, 127679. [CrossRef] [PubMed]
54. Yan, H.; Ye, Z.; Wang, Y.; He, A.; Cui, J.; Zhou, R.; Zheng, G. Dual-response behavior of chitosan humidity sensors via tailored electrode structures. *Mater. Today Commun.* **2026**, *53*, 115285. [CrossRef]
55. Nettey-Oppong, E.E.; Muhammad, R.; Ackah, E.; Yang, H.; Ali, A.; Jeong, H.W.; Kim, S.W.; Seok, Y.S.; Choi, S.H. Development of a Sustainable Flexible Humidity Sensor Based on Tenebrio molitor Larvae Biomass-Derived Chitosan. *Sensors* **2025**, *25*, 575. [CrossRef] [PubMed]
56. Kumari, P.; Kumar, A.; Yadav, A.; Gupta, G.; Gupta, G.; Shivagan, D.D.; Bapna, K. Chitosan-Based Highly Sensitive Viable Humidity Sensor for Human Health Monitoring. *ACS Omega* **2023**, *8*, 39511–39522. [CrossRef] [PubMed]
57. Cuana, R.; Nasution, T.I.; Agusnar, H.; Susilowati, A.; Lubis, N.S.; Pradana, I.S. Humidity Detection Based on Chitosan/PEO Film Sensor. *J. Phys. Conf. Ser.* **2023**, *2421*, 012038. [CrossRef]
58. Zikulnig, J.; Lengger, S.; Rauter, L.; Neumaier, L.; Carrara, S.; Kosel, J. Sustainable Printed Chitosan-Based Humidity Sensor on Flexible Biocompatible Polymer Substrate. *IEEE Sens. Lett.* **2022**, *6*, 1500804. [CrossRef]
59. Katriani, L.; Aflaha, R.; As'ari, A.H.; Nurwantoro, P.; Roto, R.; Triyana, K. Nanofiber-coated quartz crystal microbalance with chitosan overlay for highly sensitive room temperature ammonia gas sensor. *Microchem. J.* **2024**, *206*, 111532. [CrossRef]
60. Xu, J.; Bertke, M.; Li, X.; Mu, H.; Zhou, H.; Yu, F.; Hamdana, G.; Schmidt, A.; Bremers, H.; Peiner, E. Fabrication of ZnO nanorods and chitosan@ZnO nanorods on MEMS piezoresistive self-actuating silicon microcantilever for humidity sensing. *Sens. Actuators B Chem.* **2018**, *273*, 276–287. [CrossRef]
61. Xu, J.; Peiner, E. Micromachined silicon cantilever resonator-based humidity sensors for multifunctional applications. In Proceedings of the 2021 IEEE 34th International Conference on Micro Electro Mechanical Systems (MEMS), Gainesville, FL, USA, 25–29 January 2021; pp. 326–329. [CrossRef]
62. Yin, T.; Xue, C.; Li, Z.; Zhang, Y.; Xu, M.; Liu, S.; Li, L. High-performance microcantilever humidity sensor based on novel chitosan/montmorillonite composite. *Mater. Lett.* **2025**, *391*, 138529. [CrossRef]

63. Umesh, S.; Vijayan P, P.; Sambhudevan, S. Biowaste to biosensors: Comparative insights into chitosan-based nanocomposites for high-performance electrochemical sensing. *Talanta* **2026**, *307*, 129931. [CrossRef] [PubMed]
64. Suginta, W.; Khunkaewla, P.; Schulte, A. Electrochemical biosensor applications of polysaccharides Chitin and Chitosan. *Chem. Rev.* **2013**, *113*, 5458–5479. [CrossRef] [PubMed]
65. Zouaoui, F.; Bourouina-Bacha, S.; Bourouina, M.; Jaffrezic-Renault, N.; Zine, N.; Errachid, A. Electrochemical sensors based on molecularly imprinted chitosan: A review. *TrAC Trends Anal. Chem.* **2020**, *130*, 115982. [CrossRef]
66. Petrucci, R.; Pasquali, M.; Scaramuzzo, F.A.; Curulli, A. Recent advances in electrochemical chitosan-based chemosensors and biosensors: Applications in food safety. *Chemosensors* **2021**, *9*, 254. [CrossRef]
67. Bounegru, A.V.; Bounegru, I. Chitosan-Based Electrochemical Sensors for Pharmaceuticals and Clinical Applications. *Polymers* **2023**, *15*, 3539. [CrossRef] [PubMed]
68. Manna, S.; Sarkar, P.; Das, P.; Samanta, S.; Jana, S.; Nandi, G.; Sen, O. Chitosan-based nanosensors in biomedical applications: A review. *Carbohydr. Polym.* **2026**, *376*, 124824. [CrossRef] [PubMed]
69. Wu, S.; Wu, S.; Zhang, X.; Feng, T.; Wu, L. Chitosan-Based Hydrogels for Bioelectronic Sensing: Recent Advances and Applications in Biomedicine and Food Safety. *Biosensors* **2023**, *13*, 93. [CrossRef] [PubMed]
70. Ramdzan, N.S.M.; Fen, Y.W.; Anas, N.A.A.; Omar, N.A.S.; Saleviter, S. Development of biopolymer and conducting polymer-based optical sensors for heavy metal ion detection. *Molecules* **2020**, *25*, 2548. [CrossRef] [PubMed]
71. Vanderroost, M.; Ragaert, P.; Devlieghere, F.; De Meulenaer, B. Intelligent food packaging: The next generation. *Trends Food Sci. Technol.* **2014**, *39*, 47–62. [CrossRef]
72. Luo, X.; Zaitoon, A.; Lim, L.T. A review on colorimetric indicators for monitoring product freshness in intelligent food packaging: Indicator dyes, preparation methods, and applications. *Compr. Rev. Food Sci. Food Saf.* **2022**, *21*, 2489–2519. [CrossRef] [PubMed]
73. Xu, M.; Fang, D.; Kimatu, B.M.; Lyu, L.; Wu, W.; Cao, F.; Li, W. Recent advances in anthocyanin-based films and its application in sustainable intelligent food packaging: A review. *Food Control* **2024**, *162*, 110431. [CrossRef]
74. Liu, D.; Zhang, C.; Pu, Y.; Chen, S.; Liu, L.; Cui, Z.; Zhong, Y. Recent Advances in pH-Responsive Freshness Indicators Using Natural Food Colorants to Monitor Food Freshness. *Foods* **2022**, *11*, 1884. [CrossRef] [PubMed]
75. Zhai, X.; Xue, Y.; Sun, Y.; Ma, X.; Ban, W.; Marappan, G.; Tahir, H.E.; Huang, X.; Wu, K.; Chen, Z.; et al. Colorimetric Food Freshness Indicators for Intelligent Packaging: Progress, Shortcomings, and Promising Solutions. *Foods* **2025**, *14*, 2813. [CrossRef] [PubMed]
76. Bhowmik, S.; Agyei, D.; Ali, A. Smart chitosan films as intelligent food packaging: An approach to monitoring food freshness and biomarkers. *Food Packag. Shelf Life* **2024**, *46*, 101370. [CrossRef]
77. Jain, R.; Singhal, N.; Vardhan, H.; Vashistha, P.; Bist, Y.; Pandey, A.; Wagri, N.K.; Gaur, A. Polysaccharide-based functional materials for flexible electronics: A comprehensive review of synthesis strategies, functionalization, and applications. *Carbohydr. Polym. Technol. Appl.* **2025**, *12*, 101038. [CrossRef]
78. Han, W.B.; Lee, J.H.; Shin, J.-W.; Hwang, S.W. Advanced Materials and Systems for Biodegradable, Transient Electronics. *Adv. Mater.* **2020**, *32*, 2002211. [CrossRef] [PubMed]
79. Quesada-González, D.; Merkoçi, A. Mobile phone-based biosensing: An emerging "diagnostic and communication" technology. *Biosens. Bioelectron.* **2017**, *92*, 549–562. [CrossRef] [PubMed]
80. Page, M.J.; McKenzie, J.E.; Bossuyt, P.M.; Boutron, I.; Hoffmann, T.C.; Mulrow, C.D.; Shamseer, L.; Tetzlaff, J.M.; Akl, E.A.; Brennan, S.E.; et al. The PRISMA 2020 statement: An updated guideline for reporting systematic reviews. *BMJ* **2021**, *372*, n71. [CrossRef] [PubMed]
81. Page, M.J.; Moher, D.; Bossuyt, P.M.; Boutron, I.; Hoffmann, T.C.; Mulrow, C.D.; Shamseer, L.; Tetzlaff, J.M.; Akl, E.A.; Brennan, S.E.; et al. PRISMA 2020 explanation and elaboration: Updated guidance and exemplars for reporting systematic reviews. *BMJ* **2021**, *372*, n160. [CrossRef] [PubMed]
82. Anusha, J.R.; Fleming, A.T.; Kim, H.-J.; Kim, B.C.; Yu, K.-H.; Raj, C.J. Effective immobilization of glucose oxidase on chitosan submicron particles from gladius of Todarodes pacificus for glucose sensing. *Bioelectrochemistry* **2015**, *104*, 44–50. [CrossRef] [PubMed]
83. Wang, S.; Yan, H.; Zheng, H.; He, Y.; Guo, X.; Li, S.; Yang, C. Fast response humidity sensor based on chitosan/graphene oxide/tin dioxide composite. *Sens. Actuators B Chem.* **2023**, *392*, 134070. [CrossRef]

Disclaimer/Publisher's Note: The statements, opinions and data contained in all publications are solely those of the individual author(s) and contributor(s) and not of MDPI and/or the editor(s). MDPI and/or the editor(s) disclaim responsibility for any injury to people or property resulting from any ideas, methods, instructions or products referred to in the content.